UNIVERSITY OF CALIFORNIA
RIVERSIDE

A Comparative Study of the Cytotoxic and Genotoxic Effects Exerted by the Bisdioxopiperazines, Bimolane and ICRF-154

A Thesis submitted in partial satisfaction
of the requirements for the degree of

Master of Science

in

Environmental Toxicology

by

Minh-Chau Thi Vuong

December 2011

Thesis Committee:
Dr. David A. Eastmond, Chairperson
Dr. Jeffrey Bachant
Dr. Yinsheng Wang

The Thesis of Minh-Chau Thi Vuong is approved:

_____

_____

_____

Committee Chairperson

University of California, Riverside

ACKNOWLEDGEMENTS AND DEDICATION

I would like to express my gratitude to Dr. David A. Eastmond, my advisor, for all his genuine mentoring, guidance, and patience. In addition, I would like to thank you Leslie Hasegawa for her endless technical expertise help. I also would like to thank you my family for their support and love. I want to dedicate this piece of work to Jim in appreciation for his true friendship.

ABSTRACT OF THE THESIS

A Comparative Study of the Cytotoxic and Genotoxic Effects Exerted by the Bisdioxopiperazines, Bimolane and ICRF-154

by

Minh-Chau Thi Vuong
Master of Science, Graduate Program in Environmental Toxicology
University of California, Riverside, December 2011
Professor David A. Eastmond, Chairperson

Bimolane and ICRF-154 have been used for the treatment of cancer, psoriasis and uveitis in humans. Previous reports have revealed that the two drugs are topoisomerase II inhibitors, and patients treated with these agents have developed unique subtypes of secondary leukemia. Early studies have suggested that the therapeutic effects of bimolane were due to ICRF-154, an impurity present within the bimolane samples that may also be responsible for the toxic effects attributed to bimolane. To date, this hypothesis has not been tested. The objective of our study was to characterize the cytotoxic and genotoxic effects of bimolane and ICRF-154 in a series of *in vitro* tests in TK6 cells and to compare the results for the two chemicals. Bimolane and ICRF-154 were both cytotoxic exhibiting similar effects on cell proliferation across a number of endpoints. Clastogenic and

aneugenic effects of both agents were assessed using the micronucleus (MN) assay with CREST staining. These drugs induced mainly chromosome breakage and, to a lesser extent, chromosome loss at very similar frequencies. In addition, the drugs' potentials to interfere with cytokinesis were detected by measuring binucleation. Very similar responses in the induction of binucleated cells were observed with the two agents. Three assays were used to screen for numerical chromosomal abnormalities. In our flow cytometry studies, both compounds induced hypodiploidy, hyperdiploidy, and polyploidy with pronounced effects at the highest test concentration. Fluorescence *in situ* hybridization (FISH) analyses with a chromosome 7 specific centromeric DNA probe were then performed to confirm the flow cytometry results. Bimolane and ICRF-154 induced similar frequencies of numerical aberrations including hypodiploidy and a combination of hyperdiploidy and polyploidy when either of the two FISH methods were used. The results of our study demonstrate that the bimolane and ICRF-154, topo II catalytic inhibitors, exhibit very similar cytotoxic and genotoxic effects at equimolar concentrations. The results of this study strongly suggest that bimolane is efficiently converted to ICRF-154 during cell culture, and that ICRF-154 is most likely responsible for bimolane's cytotoxic, genotoxic, and, possibly, leukemogenic effects.

Tables of Contents

Page #

LIST OF FIGURES

Page #

LIST OF TABLES

Page #

Introduction

Bisdioxopiperazines were first produced in the late 1950's by chemists of Geigy Corporation as leveling agents for textile dyeing processes and as possible pharmaceuticals (Herman EH et al., 1982). Based upon the hypothesis that antineoplastic drugs are effective because they are scavengers of biometals, Creighton and co-workers initiated systematic studies of the anti-cancer properties of the potent chelating agent ethylenediaminetetraacetic acid (EDTA) and synthesis of various derivatives (Creighton AM, 1969). The investigations by Creighton and fellow workers brought about the discovery of the anti-tumor and cardioprotective properties of a class of anti-cancer drugs known as the bisdioxopiperazines at the Imperial Cancer Research Fund (ICRF) laboratories in the UK in the late 1960's (Herman EH et al., 1982; Nair RV and Witiak DT, 1988). ICRF-154, an initially synthesized product of the bisdioxopiperazines (Figure 1b), was shown to be an effective inhibitor of tumor cell growth (Creighton AM et al., 1969). The biological attributes of the bisdioxopiperazines launched research around the world into this class of therapeutics.

In 1980, Zhang and co-workers described the use of a derivative of ICRF-154 for treatment of human cancers (Zhang TM et al., 1980). This derivative, named bimolane, (1,2-bis(4-morpholinomethyl-3,5-dioxypiperozyl)ethane) (Figure 1a), was subsequently used in China as an antineoplastic drug, for psoriasis therapy, and for treatment of uveitis in humans (Zhang TM et al., 1980; Xu B et. al., 1991).

In addition to bimolane, the bisdioxopiperazines class of drugs also includes the

chemical agents razoxane (ICRF-159), ethyliminum (ICRF-154), dexrazoxane (ICRF-187), ICRF-193, and MST-16 (sobuzoxane), all of which have been examined for or employed in anti-cancer therapies (Le Serve AW and Hellmann K, 1972; Kano Y et al., 1992; Ohno R et al., 1993; Hasinoff BB 2008). Aside from its known anti-neoplastic properties, ICRF-154 was also used in China as a therapeutic treatment for psoriasis (Li YS et al., 1989; Xue Y et al., 1992; Xue Y et al., 1997). Development of therapy-related leukemia (t-AML) with short latency periods has been reported to occur in a substantial number of patients following bimolane or ICRF-154 therapy (Li YS et al., 1989; Xue Y et al., 1992; Xue Y et al., 1997). Patients with t-AML following administration of bimolane or ICRF-154 exhibited balanced chromosome translocations associated with specific FAB (French-American British classification) subtypes (Li YS et al., 1989; Xue Y et al., 1992; Xue Y et al., 1997; Pedersen-Bjergaard J and Rowley JD, 1994). These patients were typically diagnosed with acute myeloblastic leukemia (M2-FAB subtype) with the t(8;21) (q22;q22) or with acute promyelocytic leukemia (M3-FAB subtype) with the t(15;17) (q22;q12) (Li YS et al., 1989; Xue Y et al., 1992; Xue Y et al., 1997).

In earlier studies, Camerman et al. (1984) proposed that the anti-cancer and anti-psoriasis effects of bimolane could have been due to ICRF-154, which is a recognized contaminant and degradation product of bimolane (Camerman N et al., 1984). Therefore ICRF-154 may be the actual chemical component that is responsible the secondary leukemogenic effects seen with bimolane (Camerman N et al., 1984; Frantz CE et al., 1997; Pedersen-Bjergaard J and Rowley JD, 1994).

The balanced chromosomal translocations seen in the leukemic cells are believed to

occur through an induction of DNA damage mediated by inhibition of DNA topoisomerase II (topo II) and are similar to balanced chromosomal translocations involving other chromosomes that have been seen in the t-AML of patients treated with other types of topo II inhibitors (Li YS et al., 1989; Xue Y et al., 1992; Pedersen-Bjergaard J and Rowley JD, 1994). Our laboratory has previously reported that bimolane at high concentrations can inhibit topoisomerase II activity. We also identified ICRF-154 as a chemical impurity within the tested bimolane by LC-MS (Frantz CE et. al., 1997). Thus the observed topo II inhibitory effects could have been due to ICRF-154 present within the bimolane or formed through bimolane degradation.

Topo II functions as a homodimer and is required to relieve supercoiling of DNA during DNA replication and transcription (Liu LF and Wang JC, 1987; Wu HY et al., 1988; Berger JM et al., 1996; Nitiss JL, 2009). It also participates in chromosome condensation during mitosis and is required for separating newly replicated sister chromatids in cells (Hsieh TS, 1992; Nitiss JL, 2009). The role of topoisomerase II as a catalytic enzyme is to transiently introduce a double-stranded break in one DNA duplex termed the G-segment whereby the enzyme covalently links itself to the 5' end of each broken DNA strand and transports a second DNA duplex termed the T-segment through the break (Liu LF et al., 1983; Sander M and Hsieh T, 1983). This action of initiating and regulating strand passage reaction by topoisomerase II involves ATP binding and hydrolysis, and is associated with the opening and closing of the enzyme's homodimeric gates (Schoeffler AJ and Berger JM, 2008).

Our two primary goals in this investigation were to further characterize the

cytotoxic and genotoxic effects of bimolane and of ICRF-154 and to carry out comparative studies of these compounds to determine whether the cytotoxic and genotoxic potencies of bimolane differ from those of ICRF-154. This was performed by conducting a series of *in vitro* tests in the human TK6 lymphoblastoid cell line. The first method used was the cytokinesis-block micronucleus assay with CREST-antibody staining (CBMN-CREST) (Eastmond DA and Tucker JD, 1989). This method was chosen because earlier reports indicated that bimolane and bisdioxopiperazines were able to induce DNA damage in cellular systems (Chen SQ et al., 1995; Cummings J et al., 1995; Snyder RD, 2003; Jensen LH et al., 2004). The CBMN-CREST allows the effects of bimolane and ICRF-154 on cell proliferation to be assessed and the origins of the induced micronuclei (MN) to be identified (Eastmond DA and Tucker JD, 1989). Micronuclei (MN) are small extranuclear bodies that arise in once-divided cells from acentric chromosome/chromatid fragments or whole chromosomes/chromatids that are lost during mitosis and not included in the daughter nuclei (Fenech M and Morley A, 1985; Eastmond DA and Tucker JD, 1989). MN are measured as a biomarker DNA alterations resulted from clastogenic and aneugenic insults (Fenech M and Morley A, 1985; Eastmond DA and Tucker JD, 1989).

Previous studies have reported that bisdioxopiperazines can interfere with cytokinesis resulting in binucleated cells (Ishida R et al., 1991; Wheatley SP et al., 1998). As a result, the ability of bimolane and ICRF-154 to affect cytokinesis was determined by monitoring the formation of binucleated cells in the treated cultures.

In addition to determining the ability of bimolane and ICRF-154 to induce

clastogenic and aneugenic-effects using the CBMN-CREST assay, flow cytometry was used to characterize the ability of these agents to induce other types of numerical chromosomal abnormalities, similar to those seen with other bisdioxopiperazines in treated cell cultures (Taylor IW and Bleehen NM, 1978; Ishida R et al., 1994). The flow method developed by Muehlbauer and Schuler was used to monitor numerical chromosome changes induced by bimolane and ICRF-154 in mitotic populations of TK6 cells (Muehlbauer PA and Schuler MJ, 2003; Muehlbauer PA and Schuler MJ, 2005). This method is rapid and allows multiple types of numerical aberrations to be assessed simultaneously (Muehlbauer PA and Schuler MJ, 2005).

Interphase and metaphase fluorescence *in situ* hybridization (FISH) analyses with a chromosome specific centromeric DNA probe were also employed to confirm the results of the flow assay and to assess the effects of bimolane and ICRF-154 on aneuploidy and polyploidy. The two FISH methods allow the measurement of chromosomal segregation which can occur without the formation of MN (Eastmond DA and Pinkel D, 1990; Schuler M et al., 1997; Fenech M et al., 2011).

Materials and Methods

Drugs and chemicals

Bimolane (CAS no. 74550-97-3) and ICRF-154 (CAS no. 1506-47-4) were obtained from the National Cancer Institute: Chemical Carcinogen Repository. Dimethyl sulfoxide (DMSO) (CAS no. 67-68-5), cytochalasin B (CAS no. 14930-96-2), 4',6-diamidino-2-phenylindole (DAPI) (CAS no. 28718-90-3), Tween 20 (CAS no. 9005-64-

5), colcemid (CAS no. 477-30-5), propidium iodide (CAS no. 25535-16-4), and RNase A (CAS no. 9001-99-4) were all purchased from Sigma Corporation (St. Louis, MO). The CREST (calcinosis, Raynauld's phenomenon, esophageal dysfunction, sclerodactyly and telangiectasia) antibody was purchased from Antibodies Inc. (Davis, CA). Dulbecco's Phosphate-Buffered Saline, 1X (DPBS) without calcium and magnesium, utilized as buffer and sheath fluid for flow cytometer, was obtained from Invitrogen Corporation (Carlsbad, CA). Calibrite 2-Color Bead Kit used for daily calibration of the flow cytometer was purchased from BD Biosciences (San Jose, CA). The phospho-histone H3 (ser 10) 6G3 mouse antibody was acquired from Cell Signaling Technologies (Beverly, MA). Alexa Fluor 488-conjugated goat anti-mouse IgG (H+L), used for flow cytometry, was purchased from Molecular Probes (Eugene, OR). The FITC-sheep-anti-digoxigenin Fab fragments were obtained from Gibco (Carlsbad, CA).

Cell cultures

The human lymphoblastoid cell line TK6 was purchased from American Type Culture Collection (ATCC) (Manassas, VA). Cultures of TK6 cells were established in RPMI 1640 medium (Gibco; Carlsbad, CA) supplemented with 10% heat inactivated iron-supplemented calf serum (Hyclone; Logan, UT), 2 mM L-glutamine, 100 U/ml penicillin, and 100 μg/ml streptomycin (Fisher Scientific; Pittsburg, PA). All cells were maintained in a humidified incubator at 37°C in 5% CO_2: 95% air.

In vitro micronucleus assay with CREST staining

For each tested chemical, human lymphoblastoid TK6 cells were cultivated for 24 hours as 10 ml cultures with the starting cell density of ~$2.5x10^5$ cells/ml in three separate experiments. Bimolane was brought up to a final DMSO concentration of 1% and the test concentrations were 10 μM, 15 μM, and 25 μM, respectively. The treatment conditions for ICRF-154 were the same as those of bimolane.

For the *in vitro* cytokinesis-block micronucleus assay with CREST staining, cytochalasin B (4.5 μg/ml in DMSO) was added to allow cells undergoing a single cell division to be scored. Cytochalasin B treated cultures were harvested 24 hours after treatment by cytocentrifugation directly onto cleaned microscope slides at 600 r.p.m. for 5 min using a Shandon cytocentrifuge (Shandon Cytospin 2, Shandon Lipshaw Inc, Pittsburgh, PA). The slides were then fixed in 100% methanol for 10 min at room temperature and stored in a N_2 atmosphere at -20°C until further use. The MN scoring was performed as described previously (Eastmond DA and Tucker JD, 1989). A total of 1000 CREST-stained binucleated cells per test concentration per chemical in three separate experiments were analyzed for the presence of CREST staining. CREST-positive MN were determined to have originated from chromosome loss whereas CREST-negative MN were classified as having originated from chromosome breakage (Eastmond DA and Tucker JD, 1989).

The formation of binucleated cells

To measure binucleated cells in the absence of cytochalasin B, TK6 cells were cultured, harvested, and fixed as previously described for the *in vitro* micronucleus assay

without the use of cytochalasin B. A total of 200 DAPI-stained cells per test concentration per chemical in three separate experiments were analyzed for the presence of binucleated cells.

Cell proliferation and cytotoxicity

In cultures where cytochalasin-B was applied, the relative cytokinesis block proliferation index (RCBPI) was calculated as a measure of cell proliferation and cytotoxicity. RCBPI was determined by scoring 200 interphase cells per test concentration of bimolane and ICRF-154 in three separate experiments for the presence of mononucleated, binucleated, trinucleated, and tetranucleated cells (Kirsch-Volders M et al., 2003). RCBPI was calculated based upon the equation published by Kirsch-Volders and colleagues (2003) where RCBPI = [M1 + (2xM2) + 3x(M3 + M4)]/*n*. M1 to M4 represented the number of cells having one to four nuclei, respectively, and *n* was the total number of scored cells in each treatment (Kirsch-Volders M et al., 2003). To compute the percentage of RCBPI as a measurement of the percentage of cytotoxicity relative to DMSO as a solvent control, the following formula was applied: % RCBPI = 100 [$(CBPI_t - 1) / (CBPI_c - 1)$] where c denoted as control cultures and t denoted as treated cultures (Kirsch-Volders M et al., 2003; Lorge E et al., 2008).

For cultures treated in the absence of cytochalasin-B, cell proliferation and cytotoxicity were determined by calculating relative population doublings (RPDs) as follows. Population doublings (PDs) = [log(final cell count)/(initial cell count)]/[log2] (Greenwood SK et al., 2004; OECD, 2010). Relative population doublings (RPDs) =

[(no. of population doublings in treated cultures) / (no. of population doublings in control cultures) x 100] where population doublings (PDs) were expressed as the ratio of chemical treated cultures to the DMSO solvent control cultures, respectively (Lorge E et al., 2008; Greenwood SK et al., 2004). All non-cytochalasin B cultures had an initial cell count of ~$2.5x10^5$ cells/ml at the beginning of the treatment period and a final cell count at 24 hour after the treatment period was determined by automated cell counter (Coulter, Z2 Series).

Flow cytometry

For the flow assay, lymphoblastoid TK6 cells were exposed to the chemical or DMSO as previously described. Colcemid (0.075 μl/mg) was added to the flow cultures at 21 hour (3 hours prior to harvest) to accumulate mitotic cells for the flow-based assessment. Cell suspensions were fixed overnight in 70% ethanol at -20°C and were stored at -20°C until evaluation. The immunolabeling of cells for flow cytometry was performed as described previously (Muehlbauer PA and Schuler MJ, 2005). The ethanol fixative was removed following centrifugation, and then the samples were treated with 0.1% Tween 20/PBS solution for 10 minutes at room temperature followed by sequential labeling with phospho-histone H3 (ser 10) 6G3 monoclonal mouse antibody diluted 1:400 in PBS for 45 minutes in the dark at 37°C, and then with an Alexa Fluor 488 goat anti-mouse IgG (H+L) diluted 1:1000 in PBS for 45 minutes in the dark at 37°C. The flow cytometry-based process of immunolabeling with phospho-histone H3 (ser10) 6G3 mouse antibody differentiates mitotic cells from interphase cells with high specificity

(Muehlbauer PA and Schuler MJ, 2005). Before measurement, fixed mitotic cells were stained with propidium iodide (25 μg/ml) and their RNA was eliminated using a RNase A (200 μg/ml) solution. Instrumentation and gating for flow cytometry was performed as previously described by Muehlbauer and Schuler with a minor modification for gating (Muehlbauer PA and Schuler MJ, 2005); a trapezoid shaped gate was employed to more effectively include the cycling population of singlet polyploid TK6 cells while still eliminating doublets and apoptotic cells.

To assess numerical chromosome aberrations by flow, groups of 2000 mitotic cells, comprised of hypodiploid, diploid, hyperdiploid, and polyploid cells were simultaneously screened based upon their altered DNA content and immunochemical staining (Muehlbauer PA and Schuler MJ, 2005). Frequencies of individual aneuploid events were calculated by dividing the percent hypodiploidy, hyperdiploidy, and polyploidy by the total number of cells in mitosis (mitotic index) and multiplied by 100 (Muehlbauer PA and Schuler MJ, 2005).

The relative mitotic index (RMI) was used as a measure of cell proliferation and toxicity when using the flow-based method. RMI was determined as the ratio of mitotic cells or mitotic index (MI) in the treated cells to the MI of the respective DMSO solvent control multiplied by 100. MI was calculated as a division of the 2000 collected mitotic cells by the total number of mitotic and non-mitotic cells evaluated.

Fluorescence in situ hybridization studies

Human lymphoblastoid TK6 cells were cultured as described earlier. For

fluorescence *in situ* hybridization (FISH) interphase and metaphase cultures were harvested 24 hours following treatment. Colcemid (0.075 μl/mg) was added to metaphase cultures at 21 hour (3 hours before harvest) to arrest dividing TK6 cells at metaphase. At the 24-hour harvest time, interphase cultures and metaphase cultures were centrifuged, and the media aspirated. Cell suspensions were swollen in a hypotonic KCl solution (0.075 M) at room temperature for 30 min. The cell pellets were resuspended in Carnoy's fixative (3 methanol: 1 acetic acid) three times, and the fixed cells were dropped onto pre-cleaned glass slides, air dried, and stored under N_2 at -20°C until use.

Fluorescence *in situ* hybridization (FISH) with a chromosome-specific α-satellite centromeric DNA probe for chromosome 7 was used. The probe was generated and labeled as previously described (Hasegawa LS et al., 1995) and standard conditions for FISH were employed (Trask B and Pinkel D, 1990). In short, the hybridization mix included 55% formamide, 10% dextran sulfate, 1X SSC (Master Mix, MM 2.1), the digoxigenin-labeled α-satellite probe for chromosome 7 (20-100 ng), and sheared herring sperm DNA (1 mg/ml) in a total volume of 10 μl. The probe DNA for chromosome 7 was denatured for 5 min in 70% formamide 2X SSC, dehydrated in a 70%, 85%, and 100% ethanol series for 2 min each at room temperature. 10 μl of denatured probe were hybridized onto slides, which were initially maintained at 40-42°C using a slide warmer. The slides were incubated overnight in the dark at 37°C in a humidified chamber. Post hybridization washes consisting of three washes in 50% formamide 2X SSC at 37°C for 5 min per wash followed by a quick rinse in 2X SSC at room temperature. The digoxigenin-labeled probe was detected using a FITC-labeled anti-digoxigenin Fab

fragment from sheep (20 μg/ml in PNM[1]) incubated on the slide for 20 min at 37°C in humidified chamber (Rupa DS et al., 1995). The nuclei were counterstained with DAPI (2.5 μg/ml) in a phenylenediamine antifade mounting medium.

The number of hybridization-containing nuclei was determined using the scoring procedures described previously (Eastmond DA and Pinkel D, 1990). A total of 1000 interphase nuclei and a total of 500 metaphase nuclei per test concentration for each chemical agent were analyzed for numerical alterations in three independent experiments. Cells with less than two spots for chromosome 7 were classified as hypodiploidy due to loss of chromosome 7. Cells with more than two spots for chromosome 7 were categorized as a combination of hyperdiploidy resulting from gain of chromosome 7 and polyploidy resulting from an increase in the haploid complement of chromosomes. The frequencies of hypodiploidy and hyperdiploidy/polyploidy were computed as the ratio of aberrant cells to the total number of cells evaluated.

Statistical analysis

Dose-related increases in micronucleated and aneuploid/polyploid cells were determined using the Cochran-Armitage test for trend in binomial proportions (Margolin BH and Risko KJ, 1988). Following a positive response in the trend test, a one-tailed Fisher's exact test was employed to compare individual treatments against the respective controls and to compare test results for bimolane against those of ICRF-154 (Gad SC, 2006). Critical values were determined using a 0.05 probability of type I error.

[1] The abbreviation used is: PNM, 0.1 M phosphate buffer containing 5% powdered nonfat milk supernatant and 0.5% NP40.

Results

Measures of cell proliferation and cytotoxicity

To characterize the cytotoxic effects of bimolane and ICRF-154, three measures of cell proliferation: RCBPI, RPDs, and RMI were used (Figure 2). For the three endpoints, significant dose-related decreases in cell proliferation were seen ($P_{Cochran\text{-}Armitage} \leq 0.001$; Tables 1-2). RMI was the most sensitive indicator of cytotoxicity followed by RPDs and RCBPI. Significant dose-related decreases were seen at each of the test concentrations for the three measures ($P_{Fisher's} \leq 0.05$). The decreases in cell proliferation were remarkably similar for the two drugs.

Detection of chromosome breakage and chromosome loss by the in vitro micronucleus assay with CREST staining

As illustrated in Figure 3, significant dose-related increases in micronucleated cells (MNC) were also induced by bimolane and ICRF-154 ($P_{Cochran\text{-}Armitage} \leq 0.001$), with significant increases seen at each of the individual test concentrations ($P_{Fisher's} \leq 0.05$). The induced MN were formed predominantly from chromosome breakage, as evidenced by significant dose-related increases in kinetochore-negative micronuclei (K-MN). These were seen at each of the test concentrations for both compounds ($P_{Fisher's} \leq 0.05$). Similar clastogenic effects were seen for both bimolane and ICRF-154. Less pronounced but significant dose-related increases in kinetochore-positive MN, indicative of chromosome loss, were also seen for the two compounds ($P_{Cochran\text{-}Armitage} \leq 0.01$). Small but statistically significant increases were seen at all concentrations of bimolane, but only at the higher 15-25 μM test concentrations for ICRF-154 ($P_{Fisher's} \leq 0.05$). The frequency of

kinetochore-positive MN was significantly higher for ICRF-154 at the 25 μM concentration than for bimolane at the same test concentration ($P_{Fisher's} \leq 0.025$). These results indicate that bimolane and ICRF-154 induce both DNA breakage and chromosome loss.

Detection of binucleated cells induced by bimolane and ICRF-154

As shown in Figure 4, bimolane and ICRF-154 exhibited similar and statistically significant dose-related increases in the formation of binucleated cells. Significant increases were seen for each of the test concentrations for bimolane and at the higher test concentrations for ICRF-154 ($P_{Cochran-Armitage} \leq 0.001$; Tables 1-2). A particularly noticeable increase in the frequency of binucleated cells was apparent at the 25 μM concentration for both chemicals ($P_{Fisher's} \leq 0.05$). The increase in binucleated cells appeared to be slightly greater for ICRF-154 than for bimolane at this concentration. These results indicate that both chemical agents have a very similar effects in interfering with the completion of cytokinesis.

Detection of numerical chromosomal abnormalities by flow cytometry

To further assess the effects of the two chemical agents, numerical chromosome alterations were measured by flow cytometry in the bimolane- and ICRF-154-treated cells. As illustrated in Figure 5, significant dose-related increases in each of the major classes of chromosomal alterations were exerted by both bimolane and ICRF-154 ($P_{Cochran-Armitage} \leq 0.001$). Significant increases in hypodiploidy were seen at all of the test

concentrations for bimolane ($P_{Fisher's} \leq 0.05$) and at the higher (15-25 μM) test concentrations for ICRF-154 ($P_{Fisher's} \leq 0.05$). A greater induction in hypodiploidy was seen with ICRF-154 than bimolane at the 25 μM concentration ($P_{Fisher's} \leq 0.025$). Significant and dose-related increases in hyperdiploidy were also recorded for each of the test concentrations of ICRF-154 and at the 15 and 25 μM concentrations of bimolane ($P_{Fisher's} \leq 0.05$). Again, the increase in hyperdiploidy at the 25 μM concentration was greater for ICRF-154 than for bimolane ($P_{Fisher's} \leq 0.025$).

Similarly, significant dose-related increases in polyploidy were also induced by both bimolane and ICRF-154 ($P_{Cochran\text{-}Armitage} \leq 0.001$), with significant increases observed at the 15 and 25 μM concentrations ($P_{Fisher's} \leq 0.05$). Similar to what was seen for hypo- and hyperdiploidy, a more substantial increase in the frequency of polyploidy was seen for ICRF-154 at 25 μM concentration than for bimolane ($P_{Fisher's} \leq 0.025$). These results indicate that the ability of bimolane and ICRF-154 to induce hypodiploidy, hyperdiploidy, and polyploidy were very similar.

Detection of numerical chromosomal abnormalities in interphase cells FISH with a chromosome 7 probe

To confirm the results seen in the flow assay, interphase FISH with a chromosome-specific DNA probe was used to determine the number of copies of chromosome 7 present in cells following treatment with bimolane and ICRF-154. As shown in Figure 6, the two agents showed comparable dose-related trends in inducing numerical chromosomal changes ($P_{Cochran\text{-}Armitage} \leq 0.001$). Significant dose-related increases in

hypodiploidy were measured for both chemical agents, with significant increases seen for all test concentrations ($P_{Fisher's} \leq 0.05$; Figure 6).

With regard to chromosome gain, bimolane and ICRF-154 induced similar and significant dose-related increases in hyperdiploidy/polyploidy ($P_{Cochran\text{-}Armitage} \leq 0.001$), with significant increases detected at each of the individual test concentrations (Figure 6) ($P_{Fisher's} \leq 0.05$). Again, ICRF-154 was more potent in inducing hyperdiploidy/polyploidy than bimolane at the highest 25 μM test concentration ($P_{Fisher's} \leq 0.025$; Figure 6b). Similar interphase FISH results were seen at the other test concentrations for bimolane and ICRF-154. Consistent with the flow results, the interphase FISH data showed that the combined two agents produced similar levels frequency of chromosome loss as well as hyperdiploidy and polyploidy.

Detection of numerical chromosomal abnormalities in metaphase cells using FISH

FISH with the chromosome 7 specific probe was also used to detect numerical chromosome changes in cells recovered at metaphase in the cell cycle following drug treatments. As shown in Figure 7, weak hypodiploid responses were seen for both bimolane and ICRF-154. Bimolane at the test concentrations of 15-25 μM showed significant dose-related increases for chromosome loss while a weaker statistically non-significant trend for hypodiploidy was seen for ICRF-154, largely due to a slightly reduced response at the 25 μM test concentration.

For hyperdiploidy/polyploidy, similar and significant dose-related increases were seen for the two chemicals, with significant increases seen at each of the individual test

concentrations ($P_{Fisher's} \leq 0.05$; Figure 7). ICRF-154 was a more potent inducer of hyperdiploidy/polyploidy than bimolane at the 25 μM concentration ($P_{Fisher's} \leq 0.025$; Figure 7b). The overall results from FISH analyses indicate that bimolane and ICRF-154 have similar aneugenic effects. Additional information on the FISH results as well as detailed comparisons between the aneuploidy and polyploidy frequencies can be found in Appendices A-H.

Discussion

Previous research based primarily on chemical analyses, had suggested that ICRF-154, a chemical impurity present within bimolane samples, was responsible for the therapeutic effects attributed to bimolane (Camerman N et. al., 1984). If true, it is also likely that ICRF-154 would be responsible for the genotoxic and leukemogenic effects of bimolane. However to date, this hypothesis has not been tested, and currently, very limited information is available on the toxicity and genotoxicity of these two compounds. The main objective of our study was to test this hypothesis by characterizing the toxic and genotoxic effects of bimolane and ICRF-154 in a human cell line using a variety of *in vitro* tests, and comparing the results from the two compounds. The results from our *in vitro* studies clearly demonstrate that bimolane and ICRF-154 are toxic and genotoxic inducing very similar patterns of cytotoxic and chromosomal abnormalities at equimolar concentrations. The induced abnormalities included anti-proliferative and cytotoxic effects, chromosome breakage, chromosomal loss and nondisjunction, binucleation, and polyploidy.

Comparison of measures of cell proliferation and cytotoxicity

Three measures of cell proliferation and cytotoxicity were compared, specifically RCBPI, RPDs, and RMI. As illustrated in Figure 2, very similar dose-response curves were seen with bimolane and ICRF-154 with anti-proliferative effects being seen at equimolar concentrations for each of the three test endpoints. The very similar results for each of the three endpoints are consistent with our hypothesis that the cell proliferative and cytotoxic effects of bimolane are due to its conversion into ICRF-154.

In recent years, concerns have been raised about chromosome damage occurring as secondary effect due to nuclease activation in dying cells when excessive cytotoxicity occurs during an experiment (Galloway S, 2000). To address this issue, the Organisation for Economic Cooperation and Development recommends that the highest test concentration for the MN assay not exceed 55% toxicity (OECD 2010). Similarly, the most recent International Conference on Harmonisation (ICH) S2R1 draft guideline for *in vitro* genotoxicity studies recommends that inhibition of cell proliferation as measured by cell growth not be greater than about 50% (ICH, 2008). As shown in Figure 2 for each of the three measures, cytotoxicity did not exceed 50% at the 10 μM test concentrations for either bimolane or ICRF-154. At this concentration, significant genotoxic effects were seen for almost all of the chromosomal and cellular effects measured (Figures 4-6) confirming that these were not effects that occurred secondary to cytotoxicity. While higher test concentrations resulted in higher levels of cytotoxicity, it is not clear what effect cytotoxicity had on the observed results. For example, while DNA strand breakage

may occur secondary to cytotoxicity, it is not clear how the processes leading directly to cell death would lead to the increases in aneuploidy, polyploidy or binucleation that were seen at the higher doses.

Analysis of chromosome breakage by the in vitro micronucleus assay with CREST staining

As evidenced in Figure 3, bimolane and ICRF-154 are both chromosomal damaging agents inducing similar frequencies of micronuclei at equimolar test concentrations. Previous studies by Xue KX et al. (1992 a), Xue KX et al. (1992 b), and Xue KX et al. (1994) for bimolane and Snyder RD (2003) for ICRF-154 reported that the *in vitro* treatment of cells with these compounds resulted in an increase in micronuclei. However in these earlier studies, the origins of induced micronuclei were not determined. As shown in our experiments using the CREST antibody, the MN induced by these two agents originated predominantly from chromosomal breakage. Similar increases in CREST-negative micronuclei have been seen in peripheral blood cultures following treatment with bimolane (Roy SK and Eastmond DA, in press).

The bisdioxopiperazine class of topo II inhibitors that include bimolane and ICRF-154, are classified as catalytic inhibitors of topo II that inhibit the enzyme following resolution of the cleavable complex resulting in an inhibited enzyme that encompasses the DNA duplex in a closed clamp conformation (Frantz CE et al., 1997; Tanabe K et al., 1991). Given that the cleavable complex has been resolved and that the cleaved double-stranded DNA has been religated at this stage, it is not clear exactly how catalytic inhibition of the enzyme results in chromosomal breakage. However, as indicated above,

these compounds and other catalytic inhibitors of topo II have been shown to induce chromosome breakage in both cellular systems and animal models (Chen SQ et al., 1995; Cummings J et al., 1995; Wang L and Eastmond DA, 2002; Wang L et al., 2007). It is likely that DNA replication and transcription occurring in the absence of functional topo II would result in fork collapse due to stalled replication forks and an accumulation of unresolved DNA supercoiling (Ishimi Y et al., 1992; Wong ML and Hsu MT, 1990; Mondal N and Parvin JD, 2001; Nitiss JL 2009). Clastogenic effects may also occur as the chromosomes are being pulled apart by the spindle forces during anaphase, resulting in chromosome breakage (Holm C et al., 1989). The observed DNA breakage could also be due to topological impediments during chromosome condensation.

The generation of chromosomal breakage by bimolane and ICRF-154 would be expected to trigger aberrant recombination which could lead to stable structural chromosomal rearrangements, such as the specific reciprocal chromosome translocations on chromosomes 8;21 and 15;17 that have been seen in patients previously treated with bimolane, ICRF-154, and other bisdioxopiperazine compounds (Li YS et al., 1989; Tebbi CK et al., 2007; Caffrey EA et al., 1985). The balanced translocations that are present within the leukemic cells result in the fusion of genes that alter cell growth and cell differentiation, and are believed to play key roles in the development of the M2 and M3 subtypes of t-AML (Rabbitts TH, 1994). These translocations with their associated fusion gene products can, in turn, also lead to epigenetic changes that alter key regulatory factors involved in hematopoiesis, transcription, and signal transduction (Nervi C et al., 2008; Chen J et al., 2010; Tickenbrock L et al., 2011). As a result, chromosomal

breakage induced by bimolane and ICRF-154 in the hematopoietic stem cells of patients taking these could play a key initial role in the development of therapy-related leukemias induced by these agents.

Analysis of nondisjunction and chromosome loss by the in vitro micronucleus assay with CREST staining and interphase fluorescence in situ hybridization

As illustrated in Figures 3 and 6, bimolane and ICRF-154 can induce a variety of numerical chromosomal aberrations in human lymphoblastoid TK6 cells treated *in vitro* including chromosome loss and nondisjunction. CREST-positive staining showed that both compounds induced similar frequencies of micronuclei formed from chromosome loss (Figure 3). Similarly, interphase FISH using the chromosome 7 probe showed that both compounds produced very similar dose-related increases in hypodiploid and hyperdiploid cells at equimolar concentrations (Figure 6). Earlier results from Tateno H and Kamiguchi Y (2002) showed that ICRF-193, another bisdioxopiperazine induced aneuploidy in mouse oocytes *in vitro* (Tateno H and Kamiguchi Y, 2002). The induction of aneuploidy was reported to be due to an interference of ICRF-193 with sister chromatid separation during anaphase II of meiosis.

Topo II is required for the separation of sister chromatids, and it is likely that the observed increases in nondisjunction were due to the inhibition of topo II at this stage (Shamu CE and Murray AW, 1992; Gorbsky GJ, 1994; Moser SC and Swedlow JR, 2011). Sister chromatids with improper kinetochore attachments have been reported to fail to segregate properly resulting in aneuploid daughter cells (Gorbsky GJ, 1994).

Analysis polyploidy by binucleation, flow cytometry, and interphase and metaphase fluorescence in situ hybridization

As shown in Figures 4-7, both bimolane and ICRF-154 induced at least two different types of polyploidy in the treated TK6 cells. Similar increases in the recovery of binucleated cells, one type of polyploidy, were induced by bimolane and ICRF-154, again at equimolar concentrations. Xue and colleagues previously reported that bimolane caused an induction of binucleated cells (Xue et al., 1994). In addition, Ishida R and coworkers (1991) reported an induction of binucleated cells in human T-cell-derived acute lymphoblastic leukemia RPMI 8402 cells by ICRF-154. Our observations of binucleation at the 25 μM concentration of ICRF-154 in the treated TK6 cells is very similar to the results reported by Ishida R et al. (1991) in the RPMI 8402 cells at the same test concentration.

The increases in binucleation seen with the two chemical agents may be explained by the inhibition of topo II during mitosis. Earlier results from Wheatley SP et al. (1998) showed that ICRF-187 led to abnormal cytokinesis in normal rat kidney (NRK) epithelial cells *in vitro* (Wheatley SP et al., 1998). An induction in abnormal cleavage was reported to occur as a result of aberrant midzone microtubule bundles in response to the inhibition of chromosome segregation by ICRF-187 during anaphase of mitosis (Wheatley SP et al., 1998). The observed binucleation from our study may be a consequence of lagging chromosomes that interfere with cytokinesis combined with a delay in sister chromatid separation resulting in cells that exit mitosis without proper nuclear segregation.

GTPase inhibition is another possible mechanism of action that could also explain the induction of binucleated cells by bimolane and ICRF-154. A number of

bisbisdioxopiperazine compounds have recently been reported to inhibit the GTPase activity of cells (Lu DY and Lu TR, 2010). One GTPase, Rho GTPase, has been associated with cell migration through the regulation of actin cytoskeleton (Etienne-Manneville S and Hall A, 2002). Inhibition of this enzyme could impair the nuclear migration cycle that is tightly coupled to actin organization and to actin-myosin contraction, which in turn could result in an increase in binucleated cells (Etienne-Manneville S and Hall A, 2002; Parsons JT et al., 2010).

As indicated above, polyploidy in mononuclear cells was another type of abnormality induced by bimolane and ICRF-154. Interphase and metaphase FISH as well as flow-based cytometry, each showed that these compounds induced similar dose-related increases of polyploidy. Previous studies have demonstrated that cells treated with other bisdioxopiperazines have exhibited elevated frequencies of polyploidy (Taylor IW and Bleehen NM, 1978; Ishida R et al., 1994; Hasinoff BB et al., 2002). For instance, in ICRF-187 and ICRF-193-treated cells, the replicated chromosomes bypassed mitosis without chromosome segregation, resulting in polyploidy in the following cell cycle (Ishida R et al., 1994; Hasinoff BB et al., 2002; Smith PJ et al., 2007). An important function of topo II is to decatenate sister chromatids during mitosis (Shamu CE and Murray AW, 1992; Gorbsky GJ, 1994; Moser SC and Swedlow JR, 2011). A drug-related interference with the enzyme's catalytic activity during mitosis could likely lead to the increases in chromosome nondisjunction and polyploidy that were seen in treated cells.

Three different assays were employed to investigate the aneugenic and polyploidy-inducing characteristics of bimolane and ICRF-154. For each endpoint, there were

differences in the proportions of hyperdiploid and polyploid cells seen in the FISH and flow-based assays (Figures 5-7). While the exact reason for these differences are unknown, we believe that they may be due to technical issues that specifically affected the flow-based assay. Of particular note, following treatment with bimolane and ICRF-154, there appeared to be dose-related decreases in the binding of the anti-H3-P antibody to the cells, which was exhibited as a reduced separation between the mitotic and non-mitotic cells in the flow-based assay. This could have been responsible for the lower incidence of polyploidy that was seen at each test concentrations for both chemical agents when the flow results are compared to the metaphase FISH results. As topo II is involved with condensation of newly replicated sister chromatids during prophase, inhibiting topo II activity could lead to altered chromosome condensation which could potentially interfere with anti-H3-P mAb labeling (Uemura T et al., 1987; Downes CS et al., 1994; Anderson H and Roberge M, 1996; Wei Y et al., 1998). Alternatively, these compounds may interfere with H3 phosphorylation through a more direct mechanism similar to that seen with the aurora kinase inhibitors (Hsu JY et al., 2000; Morrison C et al., 2000). While we are confident that both bimolane and ICRF-154 induce polyploidy, we believe that the specific frequencies observed in the flow assay should be considered to be only approximate given the relatively weak antibody binding that was seen in the treated cells.

To confirm our flow-based results, we employed interphase and metaphase FISH methods for the assessment of the induced numerical chromosomal aberrations induced in bimolane- and ICRF-154-treated TK6 cells. While in each case, very similar results were seen for the two agents in the individual test systems, some differences were seen

between the two FISH assays used. For example, smaller increases in hypodiploidy and higher dose-related increases in hyperdiploidy/polyploidy were seen in bimolane and ICRF-154-treated metaphase cells. The reasons for these differences may be due to differential cell cycling, delayed sister chromatid separation, and/or differences in scoring criteria that have could affected the results of the two FISH assays. As an example, a 3 to 3.5-fold higher frequency in the combination of hyperdiploidy and polyploidy was seen in the metaphase FISH analysis when compared to the interphase FISH results. One possible reason that might account for these differences with the spatial overlap of hybridization signals in the interphase cells. Polyploid cells with catenated chromosomes that had by-passed mitosis would theoretically be able to resolve and decatenate those chromosomes during telophase or G1 stage of interphase. Since the chromosomes had previously been catenated, the centromeric regions of the chromosomes would lie in very close proximity in the interphase nucleus and would likely appear as a single hybridization signal during interphase FISH. As a result, these polyploidy cells would appear to be hyperdiploid, or even possibly diploid, using interphase FISH. When these cells entered into the next mitosis, the chromosomes would separate normally and the cells would be scored as polyploid cells using metaphase FISH.

As illustrated above, our comparative *in vitro* studies demonstrate that bimolane and ICRF-154 induce very similar cytotoxic and chromosomal abnormalities typically at equimolar concentrations across almost all of the endpoints measured. Very similar results were seen for chromosome breakage, chromosome loss, non-disjunction, binucleation, and the induction of polyploidy as well as the decreased antibody binding.

These results indicate that both agents act through very similar if not identical mechanisms to produce the observed cytotoxicity and genotoxicity. In conjunction with previous reports that ICRF-154 is present within bimolane samples, these results strongly suggest that bimolane is efficiently converted either enzymatically or nonenzymatically into ICRF-154 within our cell culture systems. In the few instances where significant differences were seen, they occurred at the 25 μM test concentration with the effect being greater in the ICRF-154-treated cells. This suggests that the bimolane conversion to ICRF-154 does not proceed as efficiently at higher concentrations. It should also be noted that ICRF-154 has been reported to cause t-AML with similar characteristics to those seen in bimolane-treated patients (Xue Y et al., 1992; Li YS et al., 1989).

In conclusion, both our results and those reported previously, indicate that the toxic and genotoxic effects of bimolane are due to its conversion into ICRF-154. Preliminary mass spectroscopy analyses have shown that bimolane and ICRF-154 have virtually identical spectra when dissolved in 50% acetonitrile. The measured protonated molecular ions of bimolane and ICRF-154 were 255.1096 and 255.1081, respectively (unpublished data), indicating that bimolane is readily converted into ICRF 154. Interestingly, our results with bimolane are quite similar to those reported for MST-16, another bisdioxopiperazine derivative of ICRF-154 that is used to treat adult acute T-cell leukemias in humans (Ohno R et al., 1993). MST-16 was synthesized by adding an additional chemical moiety to ICRF-154 to facilitate more efficient absorption across cell membranes (Cai JC et al., 1989). However, pharmacokinetic studies conducted by Narita and colleagues (1991) reported that ICRF-154 was the sole metabolite found within the

blood of MST-16 treated mice and that MST-16 was not detected, indicating that the parent compound was efficiently converted to ICRF-154 *in vivo*. Incubations with serum or small intestinal homogenates showed that MST-16 was rapidly converted to ICRF-154 *in vitro* (Cai JC et al., 1989; Narita T et al., 1991). Given the reported associations between bimolane, ICRF-154 and t-AML, these results suggest that patients treated with MST-16 are also likely to be at an increased risk of developing t-AML. Although MST-16 appears to be infrequently used, there is at least one report of a promyelocytic leukemia (M3) developing in patients that were previously treated with MST-16 (Okamota T et al., 2002).

References

1. Herman EH, Witiak DT, Hellmann K, Waravdekar VS. Biological properties of ICRF-159 and related bis(dioxopiperazine) compounds. Adv Pharmacol Chemother. 1982; 19: 249-90.

2. Creighton AM, Hellmann K, Whitecross S. Antitumour activity in a series of bisdiketopiperazines. Nature. 1969 Apr 26; 222(5191):384-5.

3. Nair RV, Witiak DT. The evolution of a cardioprotective antimetastatic and antitumor drug: An international adventure. J. Chem. Educ.. 1988, 65(6): 534-538.

4. Zhang TM, Chen ZY, Lin C. [Pharmacological studies on bimolane (AT-1727), a new antineoplastic agent (author's transl)]. Yao Xue Xue Bao. 1980 Oct;15(10):577-83.

5. Xu B, Noah PW, Skinner RB Jr, Bale G, Chesney TM, Rosenberg EW. Efficacy of bimolane in the Malassezia ovalis model of psoriasis. J Dermatol. 1991 Dec;18(12):707-13.

6. Le Serve AW, Hellmann K. Metastases and the normalization of tumour blood vessels by ICRF 159: a new type of drug action. Br Med J. 1972 Mar 4;1(5800):597-601.

7. Kano Y, Narita T, Suzuki K, Akutsu M, Suda K, Sakamoto S, Miura Y. The effects of ICRF-154 in combination with other anticancer agents in vitro.Br J Cancer. 1992 Aug;66(2):281-6.

8. Ohno R, Masaoka T, Shirakawa S, Sakamoto S, Hirano M, Hanada S, Yasunaga K, Yokomaku S, Mitomo Y, Nagai K, et al. Treatment of adult T-cell leukemia/lymphoma with MST-16, a new oral antitumor drug and a derivative of bis(2,6-dioxopiperazine). The MST-16 Study Group. Cancer. 1993 Apr 1;71(7):2217-21.

9. Hasinoff BB. The use of dexrazoxane for the prevention of anthracycline extravasation injury. Expert Opin Investig Drugs. 2008 Feb;17(2):217-23.

10. Li YS, Zhao YL, Jiang QP, Yang CL. Specific chromosome changes and nonoccupational exposure to potentially carcinogenic agents in acute leukemia in China. Leuk Res. 1989;13(5):367-76.

11. Xue Y, Lu D, Guo Y, Lin B. Specific chromosomal translocations and therapy-related leukemia induced by bimolane therapy for psoriasis. Leuk Res. 1992 Nov;16(11):1113-23.

12. Xue Y, Guo Y, Xie X. Translocation t(7;11)(P15;P15) in a patient with therapy-related acute myeloid leukemia following bimolane and ICRF-154 treatment for psoriasis. Leuk Res. 1997 Feb;21(2):107-9.

13. Pedersen-Bjergaard J, Rowley JD. The balanced and the unbalanced chromosome aberrations of acute myeloid leukemia may develop in different ways and may contribute differently to malignant transformation. Blood. 1994 May 15;83(10):2780-6.

14. Camerman N, Hempel A, Camerman A. Bimolane: structure determination indicates anticancer activity is attributable to ICRF-154. Science. 1984 Sep 14;225(4667):1165-6.

15. Frantz CE, Smith H, Eades DM, Grosovsky AJ, Eastmond DA. Bimolane: in vitro inhibitor of human topoisomerase II. Cancer Lett. 1997 Dec 9;120(2):135-40.

16. Liu LF, Wang JC. Supercoiling of the DNA template during transcription. Proc Natl Acad Sci U S A. 1987 Oct;84(20):7024-7.

17. Wu HY, Shyy SH, Wang JC, Liu LF. Transcription generates positively and negatively supercoiled domains in the template. Cell. 1988 May 6;53(3):433-40.

18. Berger JM, Gamblin SJ, Harrison SC, Wang JC. Structure and mechanism of DNA topoisomerase II. Nature. 1996 Jan 18; 379(6562):225-3

19. Nitiss JL. Targeting DNA topoisomerase II in cancer chemotherapy. Nat Rev Cancer. 2009 May; 9(5):338-50.

20. Hsieh TS. DNA topoisomerases. Curr Opin Cell Biol. 1992 Jun;4(3):396-400.

21. Liu LF, Rowe TC, Yang L, Tewey KM, Chen GL. Cleavage of DNA by mammalian DNA topoisomerase II. J Biol Chem. 1983 Dec 25;258(24):15365-70.

22. Sander M, Hsieh T. Double strand DNA cleavage by type II DNA topoisomerase from Drosophila melanogaster. J Biol Chem. 1983 Jul 10;258(13):8421-8.

23. Schoeffler AJ, Berger JM. DNA topoisomerases: harnessing and constraining energy to govern chromosome topology. Q Rev Biophys. 2008 Feb;41(1):41-101.

24. Eastmond DA, Tucker JD. Identification of aneuploidy-inducing agents using cytokinesis-blocked human lymphocytes and an antikinetochore antibody. Environ Mol Mutagen. 1989;13(1):34-43.

25. Chen SQ, Xue KX, Wu JZ, Ma GJ. [Mutagenic effects of bimolane]. Zhongguo Yao Li Xue Bao. 1995 Nov;16(6):531-3.

26. Cummings J, Sumner AT, Slavotinek A, Meikle I, Macpherson JS, Smyth JF. Cytogenetic evaluation of the mechanism of cell death induced by the novel anthracenyl-amino acid topoisomerase II catalytic inhibitor NU/ICRF 500. Mutat Res. 1995 Aug;344(1-2):55-62.

27. Snyder RD. Evidence from studies with intact mammalian cells that merbarone and bis(dioxopiperazine)s are topoisomerase II poisons. Drug Chem Toxicol. 2003 Feb;26(1):15-22.

28. Jensen LH, Dejligbjerg M, Hansen LT, Grauslund M, Jensen PB, Sehested M. Characterisation of cytotoxicity and DNA damage induced by the topoisomerase II-directed bisdioxopiperazine anti-cancer agent ICRF-187 (dexrazoxane) in yeast and mammalian cells. BMC Pharmacol. 2004 Dec 2;4:31.

29. Fenech M, Morley A. Solutions to the kinetic problem in the micronucleus assay. Cytobios. 1985;43:233-246.

30. Ishida R, Miki T, Narita T, Yui R, Sato M, Utsumi KR, Tanabe K, Andoh T. Inhibition of intracellular topoisomerase II by antitumor bis(2,6-dioxopiperazine) derivatives: mode of cell growth inhibition distinct from that of cleavable complex-forming type inhibitors. Cancer Res. 1991 Sep 15;51(18):4909-16.

31. Wheatley SP, O'Connell CB, Wang Y. Inhibition of chromosomal separation provides insights into cleavage furrow stimulation in cultured epithelial cells. Mol Biol Cell. 1998 Aug;9(8):2173-84.

32. Taylor IW, Bleehen NM. Razoxane-induced polyploidy. Br J Cancer. 1978 Jul;38(1):143-7.

33. Ishida R, Sato M, Narita T, Utsumi KR, Nishimoto T, Morita T, Nagata H, Andoh T. Inhibition of DNA topoisomerase II by ICRF-193 induces polyploidization by uncoupling chromosome dynamics from other cell cycle events. J Cell Biol. 1994 Sep;126(6):1341-51.

34. Muehlbauer PA, Schuler MJ. Measuring the mitotic index in chemically-treated human lymphocyte cultures by flow cytometry. Mutat Res. 2003 Jun 6;537(2):117-30.

35. Muehlbauer PA, Schuler MJ. Detection of numerical chromosomal aberrations by flow cytometry: a novel process for identifying aneugenic agents. Mutat Res. 2005 Aug 1;585(1-2):156-69.

36. Eastmond DA, Pinkel D. Detection of aneuploidy and aneuploidy-inducing agents in human lymphocytes using fluorescence in situ hybridization with chromosome-specific DNA probes. Mutat Res. 1990 Oct;234(5):303-18.

37. Schuler M, Rupa DS, Eastmond DA. A critical evaluation of centromeric labeling to distinguish micronuclei induced by chromosomal loss and breakage in vitro. Mutat Res. 1997 Aug 1;392(1-2):81-95.

38. Fenech M, Kirsch-Volders M, Natarajan AT, Surralles J, Crott JW, Parry J, Norppa H, Eastmond DA, Tucker JD, Thomas P. Molecular mechanisms of micronucleus, nucleoplasmic bridge and nuclear bud formation in mammalian and human cells. Mutagenesis. 2011 Jan;26(1):125-32.

39. Kirsch-Volders M, Sofuni T, Aardema M, Albertini S, Eastmond D, Fenech M, Ishidate M Jr, Kirchner S, Lorge E, Morita T, Norppa H, Surrallés J, Vanhauwaert A, Wakata A. Report from the in vitro micronucleus assay working group. Mutat Res. 2003 Oct 7;540(2):153-63.

40. Lorge E, Hayashi M, Albertini S, Kirkland D. Comparison of different methods for an accurate assessment of cytotoxicity in the in vitro micronucleus test. I. Theoretical aspects. Mutat Res. 2008 Aug-Sep;655(1-2):1-3.

41. Greenwood SK, Hill RB, Sun JT, Armstrong MJ, Johnson TE, Gara JP, Galloway SM. Population doubling: a simple and more accurate estimation of cell growth suppression in the in vitro assay for chromosomal aberrations that reduces irrelevant positive results. Environ Mol Mutagen. 2004;43(1):36-44. Erratum in: Environ Mol Mutagen. 2004;44(1):90.

42. OECD (2010). *In vitro Mammalian Cell Micronucleus Test*, Test Guideline No. 487. OECD Guidelines for Testing of Chemicals, OECD, Paris. See site: http://www.oecd-ilibrary.org/environment/oecd-guidelines-for-the-testing-of-chemicals-section-4-health-effects_20745788

43. Hasegawa LS, Rupa DS, Eastmond DA. A method for the rapid generation of alpha- and classical satellite probes for human chromosome 9 by polymerase chain reaction using genomic DNA and their application to detect chromosomal alterations in interphase cells. Mutagenesis. 1995 Nov;10(6):471-6.

44. Trask B, Pinkel D. Fluorescence in situ hybridization with DNA probes. Methods Cell Biol. 1990;33:383-400.

45. Rupa DS, Hasegawa L, Eastmond DA. Detection of chromosomal breakage in the 1cen-1q12 region of interphase human lymphocytes using multicolor fluorescence in

situ hybridization with tandem DNA probes. Cancer Res. 1995 Feb 1;55(3):640-5.

46. Margolin, BH and Risko, KJ. The statistical analysis of in vivo genotoxicity data: case studies of the rat hepatocyte UDS and mouse bone marrow micronucleus assays, J. Ashby, F.J. de Serres, M.D. Shelby, B.H. Margolin, M. Ishidate, G.C. Becking, Editors *Evaluation of Short-Term Tests for Carcinogens*, Vol. 1 Cambridge University Press, Cambridge, 1988.

47. Gad, SC. *Statistics and experimental design for toxicologists and pharmacologists.* 4th ed. CRC Taylor and Francis, Boca Raton, FL, London, 2006.

48. Galloway SM. Cytotoxicity and chromosome aberrations in vitro: experience in industry and the case for an upper limit on toxicity in the aberration assay. Environ Mol Mutagen. 2000;35(3):191-201.

49. ICH. 2008. Topic S2(R1). Genotoxicity: Guidance on genotoxicity testing and data interpretation for pharmaceuticals intended for human use. In International Conference on Harmonisation of Technical Requirements for Registration of Pharmaceuticals for Human Use. Harmonised tripatrite guideline EMEA/CHMP/ICH/126642/2008*, approved March 2008.*

50. Xue KX, Ma GJ, Wang S, Wang YP. [Nuclear anomaly test in human lymphocytes in vitro]. Zhongguo Yao Li Xue Bao. 1992_a Sep;13(5):464-7.

51. Xue KX, Ma G, Wu J, Shan Z. [Preliminary studies of the relationship between micronucleus formation and cell cycle. IV. Micronucleus formation induced by chemical mutagens at G0, G1, S and G2 phases of human lymphocytes]. Yi Chuan Xue Bao. 1992_b;19(1):17-21.

52. Xue KX, Ma GJ, Wu JZ. [Effects of bimolane on cell cycle cytokinesis in human lymphocytes in vitro]. Zhongguo Yao Li Xue Bao. 1994 Jan;15(1):87-9.

53. Tanabe K, Ikegami Y, Ishida R, Andoh T. Inhibition of topoisomerase II by antitumor agents bis(2,6-dioxopiperazine) derivatives. Cancer Res. 1991 Sep 15;51(18):4903-8.

54. Wang L, Eastmond DA. Catalytic inhibitors of topoisomerase II are DNA-damaging agents: induction of chromosomal damage by merbarone and ICRF-187. Environ Mol Mutagen. 2002;39(4):348-56.

55. Wang L, Roy SK, Eastmond DA. Differential cell cycle-specificity for chromosomal damage induced by merbarone and etoposide in V79 cells. Mutat Res. 2007 Mar 1;616(1-2):70-82.

56. Ishimi Y, Ishida R, Andoh T. Effect of ICRF-193, a novel DNA topoisomerase II

inhibitor, on simian virus 40 DNA and chromosome replication in vitro.Mol Cell Biol. 1992 Sep;12(9):4007-14.

57. Wong ML, Hsu MT. Involvement of topoisomerases in replication, transcription, and packaging of the linear adenovirus genome. J Virol. 1990 Feb;64(2):691-9.

58. Mondal N, Parvin JD. DNA topoisomerase IIalpha is required for RNA polymerase II transcription on chromatin templates. Nature. 2001 Sep 27;413(6854):435-8.

59. Holm C, Stearns T, Botstein D. DNA topoisomerase II must act at mitosis to prevent nondisjunction and chromosome breakage. Mol Cell Biol. 1989 Jan;9(1):159-68.

60. Tebbi CK, London WB, Friedman D, Villaluna D, De Alarcon PA, Constine LS, Mendenhall NP, Sposto R, Chauvenet A, Schwartz CL. Dexrazoxane-associated risk for acute myeloid leukemia/myelodysplastic syndrome and other secondary malignancies in pediatric Hodgkin's disease. J Clin Oncol. 2007 Feb 10;25(5):493-500.

61. Caffrey EA, Daker MG, Horton JJ. Acute myeloid leukaemia after treatment with razoxane. Br J Dermatol. 1985 Aug;113(2):131-4.

62. Rabbitts TH. Chromosomal translocations in human cancer. Nature. 1994 Nov 10;372(6502):143-9.

63. Nervi C, Fazi F, Grignani F. Oncoproteins, heterochromatin silencing and microRNAs: a new link for leukemogenesis. Epigenetics. 2008 Jan-Feb;3(1):1-4.

64. Chen J, Odenike O, Rowley JD. Leukaemogenesis: more than mutant genes. Nat Rev Cancer. 2010 Jan;10(1):23-36.

65. Tickenbrock L, Klein HU, Trento C, Hascher A, Göllner S, Bäumer N, Kuss R, Agrawal S, Bug G, Serve H, Thiede C, Ehninger G, Stadt UZ, McClelland M, Wang Y, Becker A, Koschmieder S, Berdel WE, Dugas M, Müller-Tidow C; Study Alliance Leukemia Group. Increased HDAC1 deposition at hematopoietic promoters in AML and its association with patient survival. Leuk Res. 2011 May;35(5):620-5.

66. Tateno H, Kamiguchi Y. Abnormal chromosome migration and chromosome aberrations in mouse oocytes during meiosis II in the presence of topoisomerase II inhibitor ICRF-193. Mutat Res. 2002 May 22;502(1-2):1-9.

67. Shamu CE, Murray AW. Sister chromatid separation in frog egg extracts requires DNA topoisomerase II activity during anaphase. J Cell Biol. 1992 Jun;117(5):921-34.

68. Gorbsky GJ. Cell cycle progression and chromosome segregation in mammalian cells

cultured in the presence of the topoisomerase II inhibitors ICRF-187 [(+)-1,2-bis(3,5-dioxopiperazinyl-1-yl)propane; ADR-529] and ICRF-159 (Razoxane). Cancer Res. 1994 Feb 15;54(4):1042-8.

69. Moser SC, Swedlow JR. How to be a mitotic chromosome. Chromosome Res. 2011 Apr;19(3):307-19.

70. Lu DY, Lu TR. Antimetastatic activities and mechanisms of bisdioxopiperazine compounds. Anticancer Agents Med Chem. 2010 Sep;10(7):564-70.

71. Etienne-Manneville S, Hall A. Rho GTPases in cell biology. Nature. 2002 Dec 12;420(6916):629-35.

72. Parsons JT, Horwitz AR, Schwartz MA. Cell adhesion: integrating cytoskeletal dynamics and cellular tension. Nat Rev Mol Cell Biol. 2010 Sep;11(9):633-43.

73. Hasinoff BB, Takeda K, Ferrans VJ, Yu ZX. The doxorubicin cardioprotective agent dexrazoxane (ICRF-187) induces endopolyploidy in rat neonatal myocytes through inhibition of DNA topoisomerase II. Anticancer Drugs. 2002 Mar;13(3):255-8.

74. Smith PJ, Marquez N, Wiltshire M, Chappell S, Njoh K, Campbell L, Khan IA, Silvestre O, Errington RJ. Mitotic bypass via an occult cell cycle phase following DNA topoisomerase II inhibition in p53 functional human tumor cells. Cell Cycle. 2007 Aug 15;6(16):2071-81.

75. Uemura T, Ohkura H, Adachi Y, Morino K, Shiozaki K, Yanagida M. DNA topoisomerase II is required for condensation and separation of mitotic chromosomes in S. pombe. Cell. 1987 Sep 11;50(6):917-25.

76. Downes CS, Clarke DJ, Mullinger AM, Giménez-Abián JF, Creighton AM, Johnson RT. A topoisomerase II-dependent G2 cycle checkpoint in mammalian cells. Nature. 1994 Dec 1;372(6505):467-70.

77. Anderson H, Roberge M. Topoisomerase II inhibitors affect entry into mitosis and chromosome condensation in BHK cells. Cell Growth Differ. 1996 Jan;7(1):83-90.

78. Wei Y, Mizzen CA, Cook RG, Gorovsky MA, Allis CD. Phosphorylation of histone H3 at serine 10 is correlated with chromosome condensation during mitosis and meiosis in Tetrahymena. Proc Natl Acad Sci U S A. 1998 Jun 23;95(13):7480-4.

79. Hsu JY, Sun ZW, Li X, Reuben M, Tatchell K, Bishop DK, Grushcow JM, Brame CJ, Caldwell JA, Hunt DF, Lin R, Smith MM, Allis CD. Mitotic phosphorylation of histone H3 is governed by Ipl1/aurora kinase and Glc7/PP1 phosphatase in budding yeast and nematodes. Cell. 2000 Aug 4;102(3):279-91.

80. Morrison C, Henzing AJ, Jensen ON, Osheroff N, Dodson H, Kandels-Lewis SE, Adams RR, Earnshaw WC. Proteomic analysis of human metaphase chromosomes reveals topoisomerase II alpha as an Aurora B substrate. Nucleic Acids Res. 2002 Dec 1;30(23):5318-27.

81. Cai JC, Shu HL, Tang CF, Komatsu T, Matsuno T, Narita T, Yaguchi S, Koide Y, Takase M. Synthesis and antitumor properties of N1-acyloxymethyl derivatives of bis(2,6-dioxopiperazines). Chem Pharm Bull (Tokyo). 1989 Nov;37(11):2976-83.

82. Narita T, Koide Y, Yaguchi S, Kimura S, Izumisawa Y, Takase M, Inaba M, Tsukagoshi S. Antitumor activities and schedule dependence of orally administered MST-16, a novel derivative of bis(2,6-dioxopiperazine). Cancer Chemother Pharmacol. 1991;28(4):235-40.

83. Okamoto T, Okada M, Wakae T, Mori A, Takatsuka H, Kakishita E. Secondary acute promyelocytic leukemia in a patient with non-Hodgkin's lymphoma treated with VP-16 and MST-16. Int J Hematol. 2002 Jan;75(1):107-8.

(a)

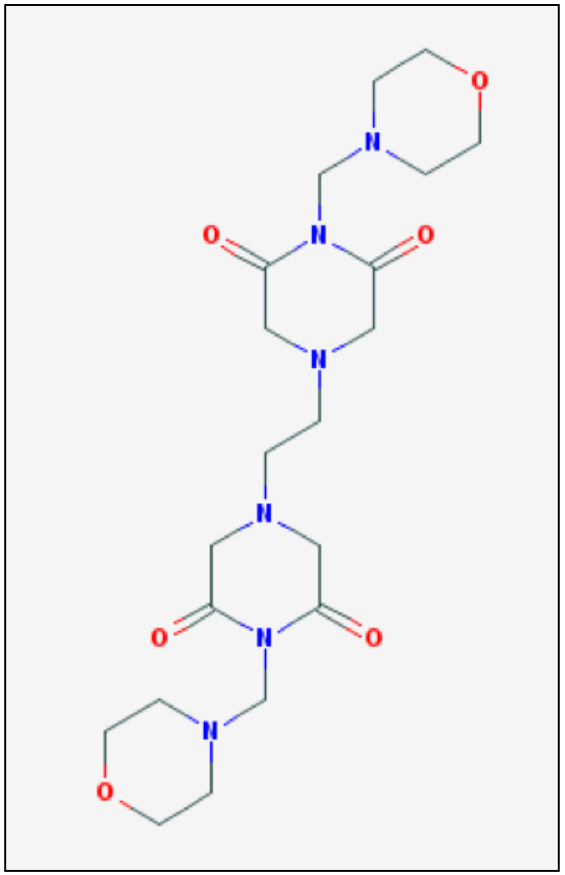

(b)

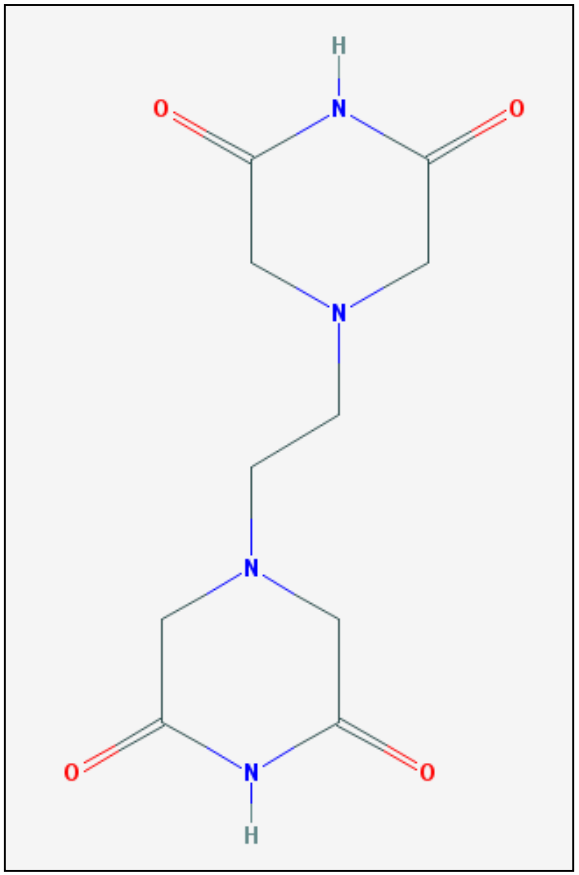

Figure 1. The chemical structures of (a) bimolane and (b) ICRF-154. Images adopted from PubChem Compound.

(a)

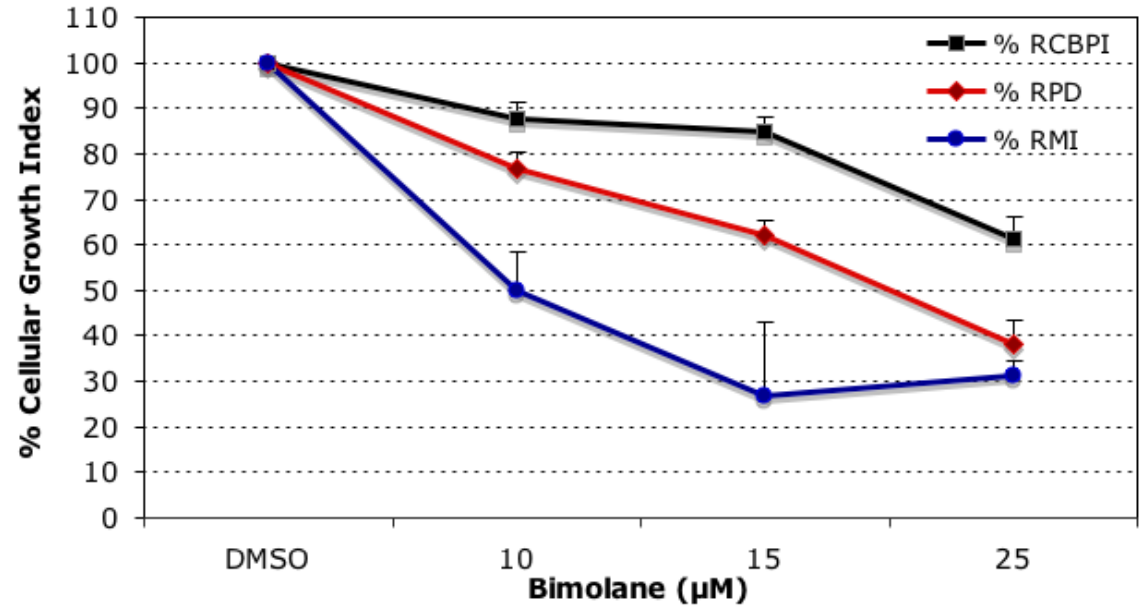

(b)

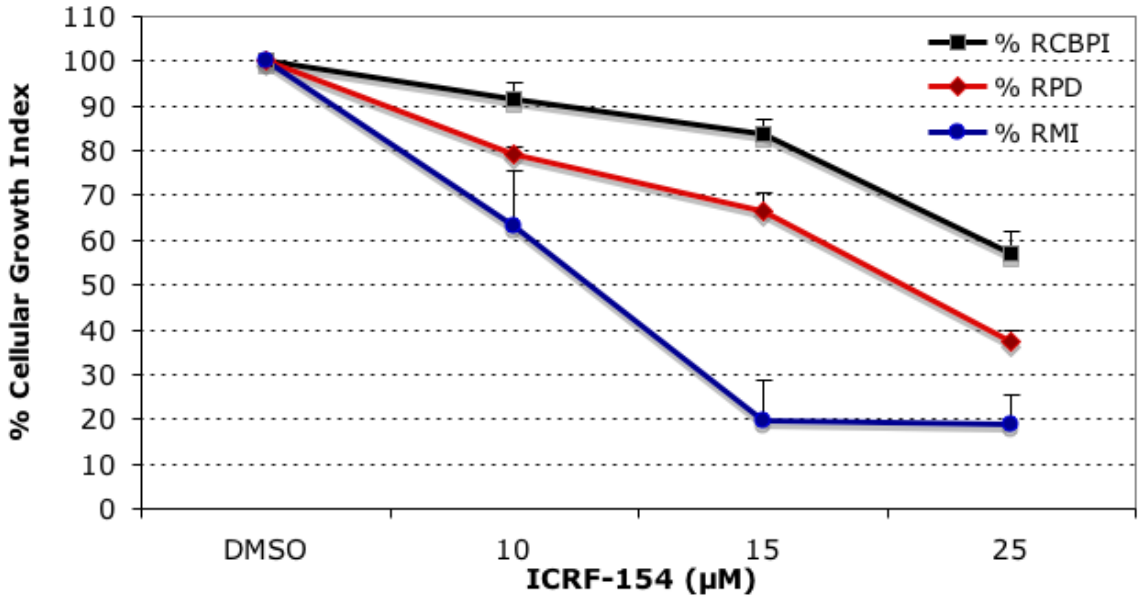

Figure 2. Measures of cell proliferation and cytotoxicity by RCBPI, RPDs, and RMI in TK6 cells treated with (a) bimolane or (b) ICRF-154 for 24 hr. Results averaged from three independent experiments. Cultures treated with each chemical significantly different by Fisher's exact test at $p \leq 0.05$ vs controls.

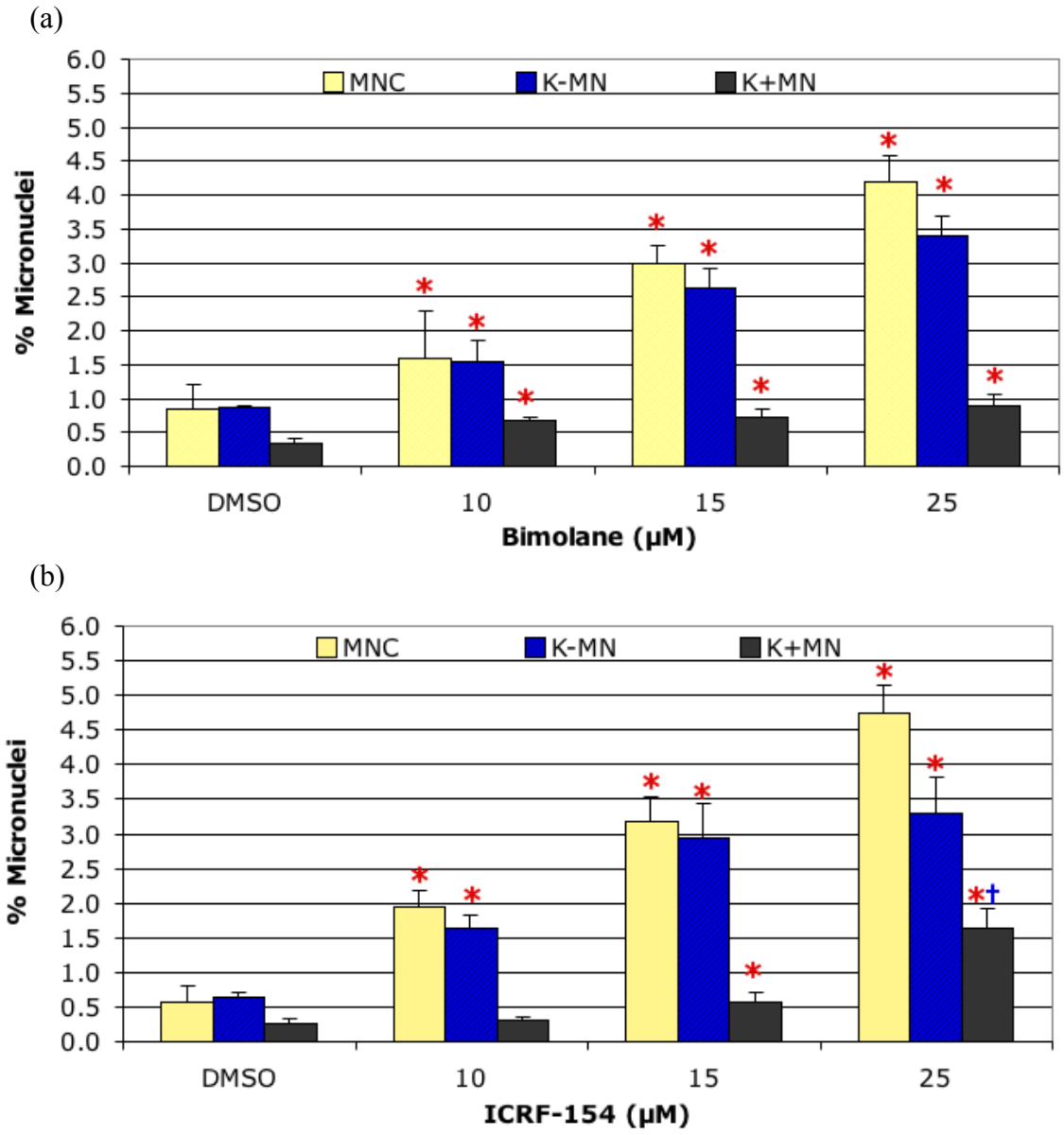

Figure 3. Frequencies of micronucleated cells (MNC), CREST-negative micronuclei, and CREST-positive micronuclei (K+MN) in TK6 cells treated with (a) bimolane or (b) ICRF-154 for 24 hr. Results averaged from three independent experiments. Asterisk represents significant increases vs controls (Fisher's exact test; $p \leq 0.05$). Cross represents significant difference between the respective bimolane and ICRF-154 test concentrations (Fisher's exact test; $p \leq 0.025$).

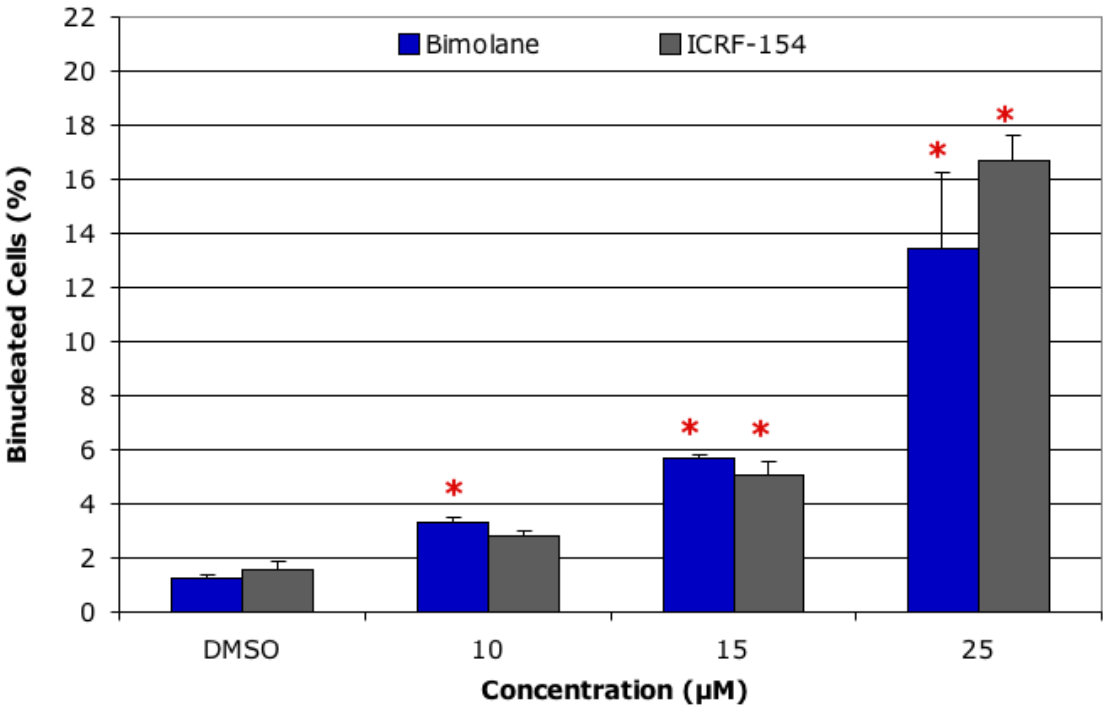

Figure 4. Frequencies of binucleated cells (BNC) in TK6 cells treated with bimolane or ICRF-154 for 24 hr. Results averaged from three independent experiments. Asterisk represents significant increases vs controls (Fisher's exact test; $p \leq 0.05$).

(a)

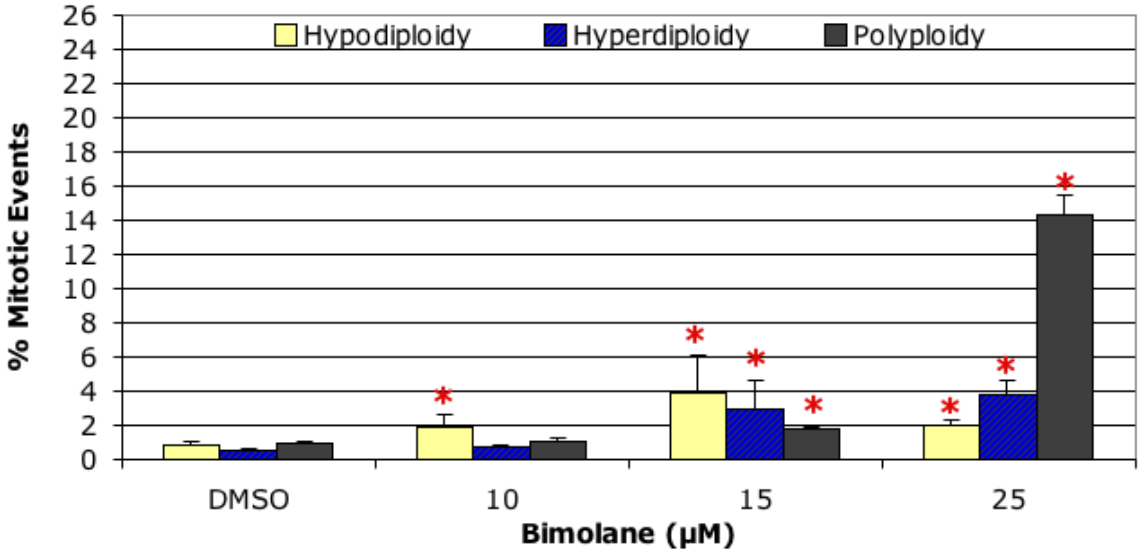

(b)

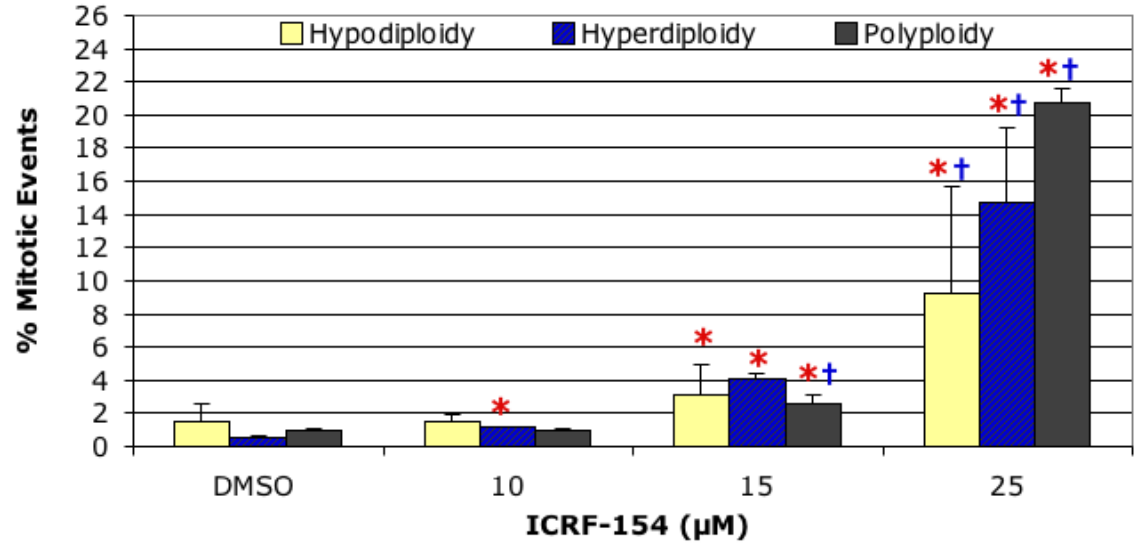

Figure 5. Numerical chromosomal aberrations measured by flow cytometry. Aberrations were computed as a percentage of 2,000 gated mitotic events in TK6 cultures treated with (a) bimolane or (b) ICRF-154 for 24 hr. Results averaged from three independent experiments. Asterisk represents significant increases vs controls (Fisher's exact test; $p \leq 0.05$). Cross represents significant difference between the respective bimolane and ICRF-154 test concentrations (Fisher's exact test; $p \leq 0.025$).

(a)

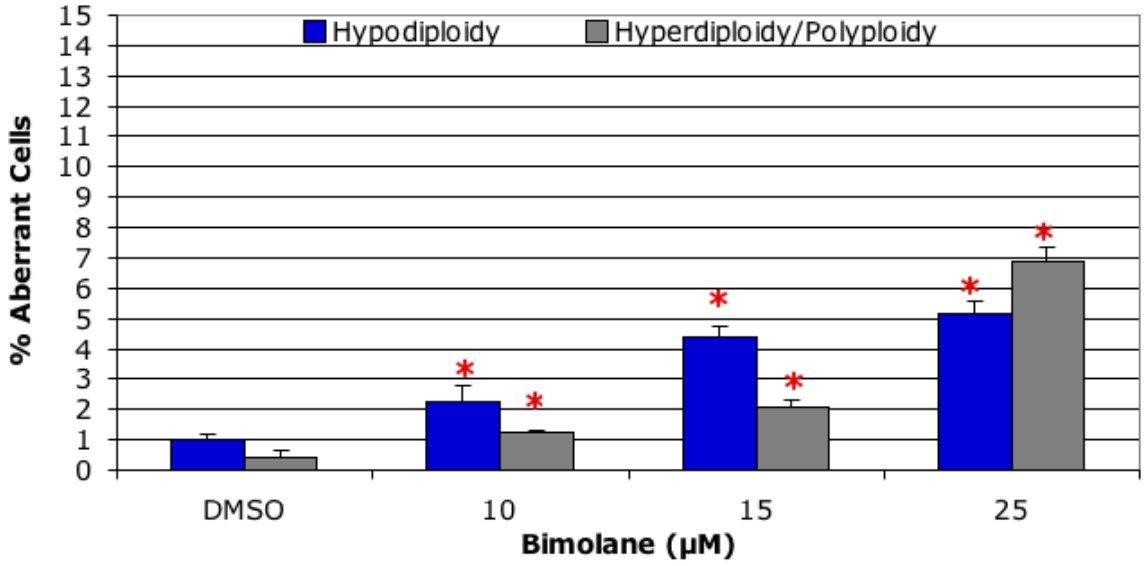

(b)

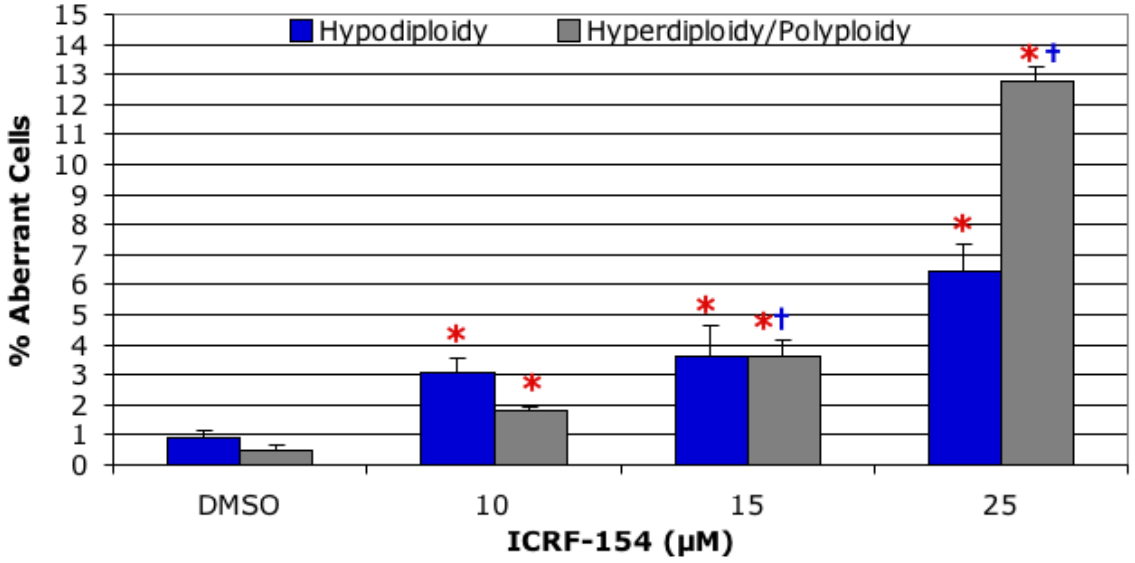

Figure 6. Frequencies of numerical chromosomal aberrations in interphase nuclei determined by FISH in TK6 cells treated with (a) bimolane or (b) ICRF-154 for 24 hr. Results averaged from three independent experiments. Asterisk represents significant increases vs controls (Fisher's exact test; $p \leq 0.05$). Cross represents significant difference between the respective bimolane and ICRF-154 test concentrations (Fisher's exact test; $p \leq 0.025$).

(a)

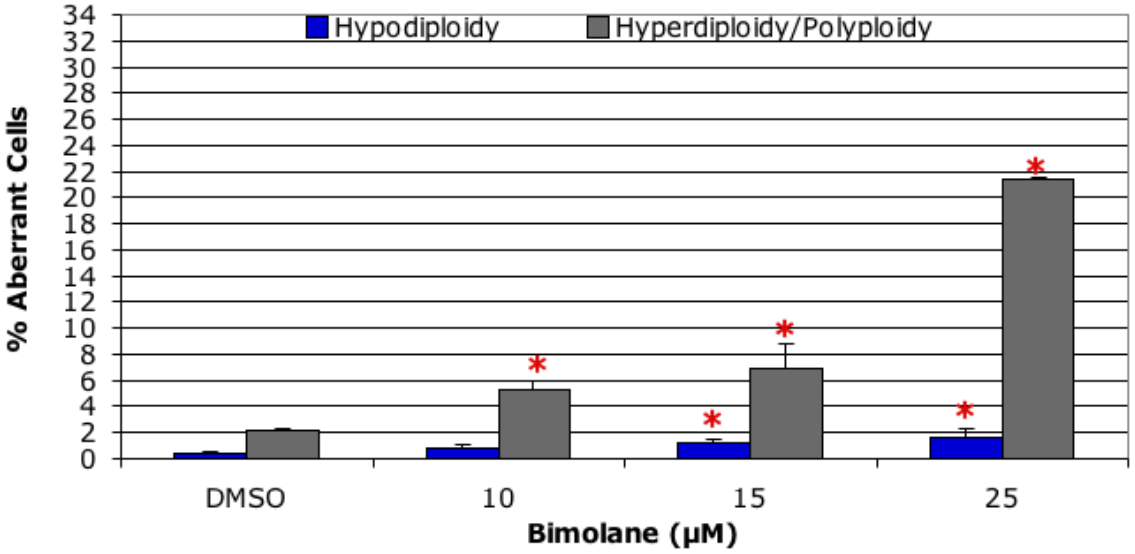

(b)

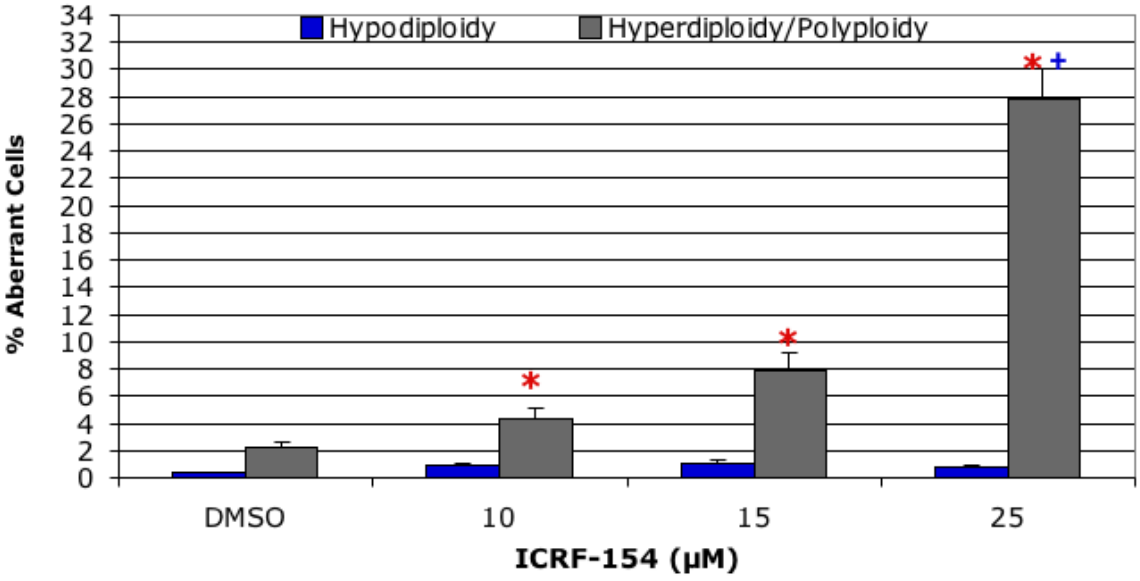

Figure 7. Frequencies of numerical chromosomal aberrations in metaphase nuclei determined FISH in TK6 cells treated with (a) bimolane or (b) ICRF-154 for 24 hr. Results averaged from three independent experiments. Asterisk represents significant increases vs controls (Fisher's exact test; $p \leq 0.05$). Cross represents significant difference between the respective bimolane and ICRF-154 test concentrations (Fisher's exact test; $p \leq 0.025$).

Table 1. Dose-related increases in cell proliferation and cytotoxicity, micronuclei, and numerical chromosomal aberrations were determined using the Cochran-Armitage test for trend. Results from the trend test were classified as positive trend ($p \leq 0.001$; $p \leq 0.01$; $p \leq 0.05$) and no trend ($p \geq 0.05$).

Bimolane	Cytotoxic and genotoxic endpoints	Z-score	P-value	Result
Cell proliferation and cytotoxicity	Relative cytokinesis-block proliferation index (RCBPI)	12.7	$p \leq 0.001$	Positive Trend
	Relative population doublings (RPDs)	14.7	$p \leq 0.001$	Positive Trend
	Relative mitotic index (RMI)	17.6	$p \leq 0.001$	Positive Trend
MN assay	Micronucleated cells (MNC) with cytochalasin B	7.65	$p \leq 0.001$	Positive Trend
	CREST-negative micronuclei (K-MN) with cytochalasin B	7.14	$p \leq 0.001$	Positive Trend
	CREST-positive micronuclei (K+MN) with cytochalasin B	2.74	$p \leq 0.01$	Positive Trend
	Binucleated cells (BNC)	9.06	$p \leq 0.001$	Positive Trend
Interphase FISH	0 spot for chromosome no.7	5.28	$p \leq 0.001$	Positive Trend
	1 spot (monosomy) for chromosome no.7	8.62	$p \leq 0.001$	Positive Trend
	Hypodiploidy (0 and 1 spot) for chromosome no. 7	9.50	$p \leq 0.001$	Positive Trend
	3 spots (trisomy) for chromosome no.7	10.5	$p \leq 0.001$	Positive Trend
	4 spots (tetrasomy) for chromosome no.7	11.6	$p \leq 0.001$	Positive Trend
	Hyperdiploidy/polyploidy (3 to > 4 spots)	15.7	$p \leq 0.001$	Positive Trend
Metaphase FISH	0 spot for chromosome no.7	1.39	$p > 0.05$	No Trend
	1 spot (monosomy) for chromosome no.7	3.26	$p \leq 0.001$	Positive Trend
	Hypodiploidy (0 and 1 spot)	3.41	$p \leq 0.001$	Positive Trend
	3 spots (trisomy) for chromosome no.7	3.29	$p \leq 0.001$	Positive Trend
	4 spots (tetrasomy) for chromosome no.7	18.8	$p \leq 0.001$	Positive Trend
	Hyperdiploidy/polyploidy (3 to > 4 spots)	18.6	$p \leq 0.001$	Positive Trend

Bimolane	Cytotoxic and genotoxic endpoints	Z-score	P-value	Result
Flow-based cytometry	Hypodiploidy	5.62	$p \leq 0.001$	Positive Trend
	Hyperdiploidy	14.1	$p \leq 0.001$	Positive Trend
	Polyploidy	34.9	$p \leq 0.001$	Positive Trend

Table 2. Dose-related increases in cell proliferation and cytotoxicity, micronuclei, and numerical chromosomal aberrations were determined using the Cochran-Armitage test for trend. Results from the trend test were classified as positive trend ($p \leq 0.001$; $p \leq 0.01$; $p \leq 0.05$) and no trend ($p \geq 0.05$).

ICRF-154	Cytotoxic and genotoxic endpoints	Z-score	P-value	Result
Cell proliferation and cytotoxicity	Relative cytokinesis-block proliferation index (RCBPI)	14.2	$p \leq 0.001$	Positive Trend
	Relative population doublings (RPDs)	14.7	$p \leq 0.001$	Positive Trend
	Relative mitotic index (RMI)	21.6	$p \leq 0.001$	Positive Trend
MN assay	Micronucleated cells (MNC) with cytochalasin B	9.68	$p \leq 0.001$	Positive Trend
	CREST-negative micronuclei (K-MN) with cytochalasin B	7.47	$p \leq 0.001$	Positive Trend
	CREST-positive micronuclei (K+MN) with cytochalasin B	6.22	$p \leq 0.001$	Positive Trend
	Binucleated cells (BNC)	10.6	$p \leq 0.001$	Positive Trend
Interphase FISH	0 spot for chromosome no.7	6.45	$p \leq 0.001$	Positive Trend
	1 spot (monosomy) for chromosome no.7	10.0	$p \leq 0.001$	Positive Trend
	Hypodiploidy (0 and 1 spot) for chromosome no.7	11.7	$p \leq 0.001$	Positive Trend
	3 spots (trisomy) for chromosome no.7	12.3	$p \leq 0.001$	Positive Trend
	4 spots (tetrasomy) for chromosome no.7	19.3	$p \leq 0.001$	Positive Trend
	Hyperdiploidy/polyploidy (3 to > 4 spots)	22.8	$p \leq 0.001$	Positive Trend
Metaphase FISH	0 spot for chromosome no.7	0.00	$p > 0.05$	No Trend
	1 spot (monosomy) for chromosome no.7	1.37	$p > 0.05$	No Trend
	Hypodiploidy (0 and 1 spot) for chromosome no.7	1.37	$p > 0.05$	No Trend
	3 spots (trisomy) for chromosome no.7	3.39	$p \leq 0.001$	Positive Trend
	4 spots (tetrasomy) for chromosome no.7	23.3	$p \leq 0.001$	Positive Trend
	Hyperdiploidy/polyploidy (3 to > 4 spots)	23.0	$p \leq 0.001$	Positive Trend

ICRF-154	Cytotoxic and genotoxic endpoints	Z-score	P-value	Result
Flow-based cytometry	Hypodiploidy	22.6	$p \leq 0.001$	Positive Trend
	Hyperdiploidy	25.9	$p \leq 0.001$	Positive Trend
	Polyploidy	44.3	$p \leq 0.001$	Positive Trend

Appendix A. Fluorescence *in situ* hybridization (FISH) with a chromosome-specific DNA probe for the centromere of chromosome 7 was used to determine the frequencies of numerical chromosomal aberrations in TK6 cells treated with bimolane for 24 h. Data averaged from three independent experiments.

Bimolane (μM)	Interphases Scored	Numerical Chromosomal Aberrations (%)					
		0 Spot	1 Spot (Monosomy for No. 7)	Hypodiploidy (0 and 1 Spot)	3 Spots (Trisomy for No. 7)	4 Spots (Tetrasomy for No. 7)	Hyperdiploidy Polyploidy (3 to > 4 Spots) [a]
DMSO	3000	0.00 ± 0.00	1.00 ± 0.35	1.00 ± 0.35	0.23 ± 0.25	0.20 ± 0.10	0.43 ± 0.35
10	3102	0.10 ± 0.10	2.15 ± 0.85	2.25 ± 0.88	0.78 ± 0.13	0.47 ± 0.06	1.23 ± 0.16
15	3000	0.70 ± 0.30	3.70 ± 0.66	4.40 ± 0.61	1.47 ± 0.46	0.57 ± 0.15	2.07 ± 0.38
25	3000	0.73 ± 0.64	4.43 ± 0.06	5.17 ± 0.67	3.43 ± 0.66	3.27 ± 0.29	6.86 ± 0.86

Red = Statistically significant by Fisher's exact test at $p \leq 0.05$ for comparison of chemical treatments against controls.
[a] Includes cells with > 4 hybridization spots.

Appendix B. Fluorescence *in situ* hybridization (FISH) with a chromosome-specific DNA probe for the centromere of chromosome 7 was used to determine the frequencies of numerical chromosomal aberrations in TK6 cells treated with ICRF-154 for 24 h. Data averaged from three independent experiments.

ICRF-154 (μM)	Interphases Scored	Numerical Chromosomal Aberrations (%)					
		0 Spot	1 Spot (Monosomy for No. 7)	Hypodiploidy (0 and 1 Spot)	3 Spots (Trisomy for No. 7)	4 Spots (Tetrasomy for No. 7)	Hyperdiploidy Polyploidy (3 to > 4 Spots) [a]
DMSO	3000	0.00 ± 0.00	0.90 ± 0.40	0.90 ± 0.40	0.43 ± 0.31	0.03 ± 0.06	0.47 ± 0.32
10	3011	0.23 ± 0.25	2.83 ± 0.91	3.06 ± 0.82	1.20 ± 0.20	0.53 ± 0.06	1.83 ± 0.16
15	3001	0.57 ± 0.32	3.03 ± 1.51	3.60 ± 1.82	1.90 ± 0.36	1.63 ± 0.55 †	3.63 ± 0.91 †
25	3000	1.11 ± 0.27	5.37 ± 1.60	6.47 ± 1.56	4.97 ± 0.46 †	7.43 ± 0.83 †	12.8 ± 0.80 †

Red = Statistically significant by Fisher's exact test at $p \leq 0.05$ for comparison of chemical treatments against controls.
† = Statistically significant by Fisher's exact test at $p \leq 0.025$ for direct comparison of bimolane against ICRF-154 concentrations.
[a] Includes cells with > 4 hybridization spots.

Appendix C. Fluorescence *in situ* hybridization (FISH) with a chromosome-specific DNA probe for the centromere of chromosome 7 was used to determine the frequencies of numerical chromosomal aberrations in TK6 cells treated with bimolane for 24 h. Data averaged from three independent experiments.

Bimolane (μM)	Metaphases Scored	Numerical Chromosomal Aberrations (%)					
		0 Spot	1 Spot (Monosomy for No. 7)	Hypodiploidy (0 and 1 Spot)	3 Spots (Trisomy for No. 7)	4 Spots (Tetrasomy for No. 7)	Hyperdiploidy Polyploidy (3 to > 4 Spots) [a]
DMSO	1522	0.00 ± 0.00	0.39 ± 0.20	0.39 ± 0.20	0.72 ± 0.50	1.28 ± 0.73	2.11 ± 0.35
10	1500	0.00 ± 0.00	0.87 ± 0.42	0.87 ± 0.42	1.73 ± 0.99	3.19 ± 0.48	5.27 ± 1.29
15	1500	0.00 ± 0.00	1.20 ± 0.60	1.20 ± 0.60	1.73 ± 1.29	4.60 ± 1.83	6.94 ± 3.32
25	1508	0.07 ± 0.11	1.52 ± 1.16	1.59 ± 1.24	2.26 ± 0.91	17.5 ± 1.54	21.4 ± 0.17

Red = Statistically significant by Fisher's exact test at $p \leq 0.05$ for comparison of chemical treatments against controls.
[a] Includes cells with > 4 hybridization spots.

Appendix D. Fluorescence *in situ* hybridization (FISH) with a chromosome-specific DNA probe for the centromere of chromosome 7 was used to determine the frequencies of numerical chromosomal aberrations in TK6 cells treated with ICRF-154 for 24 h. Data averaged from three independent experiments.

ICRF-154 (μM)	Metaphases Scored	Numerical Chromosomal Aberrations (%)					
		0 Spot	1 Spot (Monosomy for No. 7)	Hypodiploidy (0 and 1 Spot)	3 Spots (Trisomy for No. 7)	4 Spots (Tetrasomy for No. 7)	Hyperdiploidy Polyploidy (3 to > 4 Spots) [a]
DMSO	1500	0.00 ± 0.00	0.33 ± 0.12	0.33 ± 0.12	0.80 ± 0.53	1.34 ± 0.38	2.27 ± 0.70
10	1500	0.00 ± 0.00	0.87 ± 0.31	0.87 ± 0.31	1.73 ± 1.40	2.49 ± 0.51	4.33 ± 1.36
15	1500	0.00 ± 0.00	1.07 ± 0.42	1.07 ± 0.42	1.93 ± 0.81	5.30 ± 1.06	7.93 ± 2.21
25	1500	0.00 ± 0.00	0.73 ± 0.31	0.73 ± 0.31	2.39 ± 0.34	24.4 ± 3.37 †	27.8 ± 3.92 †

Red = Statistically significant by Fisher's exact test at $p \leq 0.05$ for comparison of chemical treatments against controls.
† = Statistically significant by Fisher's exact test at $p \leq 0.025$ for direct comparison of bimolane against ICRF-154 concentrations.
[a] Includes cells with > 4 hybridization spots.

Appendix E. Comparison of the frequency of chromosome loss determined in the four test systems following bimolane treatments.

Bimolane (µM)	Numerical Chromosomal Aberrations (%)			
	K+MN CBMN-CREST	Hypodiploidy Flow Cytometry	Hypodiploidy Interphase FISH	Hypodiploidy Metaphase FISH
DMSO	0.33 ± 0.15	0.87 ± 0.35	1.00 ± 0.35	0.39 ± 0.20
10	0.67 ± 0.12	1.93 ± 1.28	2.25 ± 0.88	0.87 ± 0.42
15	0.73 ± 0.21	3.90 ± 3.74	4.40 ± 0.61	1.20 ± 0.60
25	0.90 ± 0.26	2.00 ± 0.46	5.17 ± 0.67	1.59 ± 1.24

Red = Statistically significant by Fisher's exact test at $p \leq 0.05$ for comparison of chemical treatments against controls.

Appendix F. Comparison of the frequency of chromosome loss determined in the four test systems following ICRF-154 treatments.

	Numerical Chromosomal Aberrations (%)			
ICRF-154 (μM)	K+MN CBMN-CREST	Hypodiploidy Flow Cytometry	Hypodiploidy Interphase FISH	Hypodiploidy Metaphase FISH
DMSO	0.27 ± 0.12	1.47 ± 1.95	0.90 ± 0.40	0.33 ± 0.12
10	0.30 ± 0.10	1.50 ± 0.75	3.06 ± 0.82	0.87 ± 0.31
15	0.57 ± 0.25	3.07 ± 3.28	3.60 ± 1.82	1.07 ± 0.42
25	1.63 ± 0.50 †	9.23 ± 11.2 †	6.47 ± 1.56	0.73 ± 0.31

Red = Statistically significant by Fisher's exact test at $p \leq 0.05$ for comparison of chemical treatments against controls.
† = Statistically significant by Fisher's exact test at $p \leq 0.025$ for direct comparison of bimolane against ICRF-154 concentrations.

Appendix G. Comparison of the frequency of hyperdiploidy and polyploidy determined in the three test systems following bimolane treatments.

	Numerical Chromosomal Aberrations (%)			
Bimolane (µM)	Hyperdiploidy Flow Cytometry	Polyploidy Flow Cytometry	Hyperdiploidy/Polyploidy Interphase FISH	Hyperdiploidy/Polyploidy Metaphase FISH
DMSO	0.55 ± 0.13	0.95 ± 0.10	0.43 ± 0.35	2.11 ± 0.35
10	0.78 ± 0.08	1.03 ± 0.34	1.23 ± 0.16	5.27 ± 1.29
15	2.95 ± 2.91	1.78 ± 0.15	2.07 ± 0.38	6.94 ± 3.32
25	3.82 ± 1.48	14.3 ± 2.07	6.86 ± 0.86	21.4 ± 0.17

Red = Statistically significant by Fisher's exact test at $p \leq 0.05$ for comparison of chemical treatments against controls.

Appendix H. Comparison of the frequency of hyperdiploidy and polyploidy determined in the three test systems following ICRF-154 treatments.

ICRF-154 (μM)	Numerical Chromosomal Aberrations (%)			
	Hyperdiploidy Flow Cytometry	Polyploidy Flow Cytometry	Hyperdiploidy/Polyploidy Interphase FISH	Hyperdiploidy/Polyploidy Metaphase FISH
DMSO	0.55 ± 0.23	0.97 ± 0.23	0.47 ± 0.32	2.27 ± 0.70
10	1.17 ± 0.08	1.00 ± 0.18	1.83 ± 0.16	4.33 ± 1.36
15	4.05 ± 0.68	2.55 ± 0.93 †	3.63 ± 0.91 †	7.93 ± 2.21
25	14.7 ± 7.73 †	20.7 ± 1.58 †	12.8 ± 0.80 †	27.8 ± 3.92 †

Red = Statistically significant by Fisher's exact test at $p \leq 0.05$ for comparison of chemical treatments against controls.
† = Statistically significant by Fisher's exact test at $p \leq 0.025$ for direct comparison of bimolane against ICRF-154 concentrations.